

Residual-based Chebyshev filtered subspace iteration for sparse Hermitian eigenvalue problems tolerant to inexact matrix-vector products

Nikhil Kodali, Kartick Ramakrishnan, Phani Motamarri*

^aMATRIX Lab, Department of Computational and Data Sciences, Indian Institute of Science, CV Raman Road, Bengaluru, 560012, Karnataka, India

Abstract

Chebyshev Filtered Subspace Iteration (ChFSI) has been widely adopted for computing a small subset of extreme eigenvalues in large sparse matrices. This work introduces a residual-based reformulation of ChFSI, referred to as R-ChFSI, designed to accommodate inexact matrix-vector products while maintaining robust convergence properties. By reformulating the traditional Chebyshev recurrence to operate on residuals rather than eigenvector estimates, the R-ChFSI approach effectively suppresses the errors made in matrix-vector products, improving the convergence behavior for both standard and generalized eigenproblems. This ability of R-ChFSI to be tolerant to inexact matrix-vector products allows one to incorporate approximate inverses for large-scale generalized eigenproblems, making the method particularly attractive where exact matrix factorizations or iterative methods become computationally expensive for evaluating inverses. It also allows us to compute the matrix-vector products in lower-precision arithmetic allowing us to leverage modern hardware accelerators. Through extensive benchmarking, we demonstrate that R-ChFSI achieves desired residual tolerances while leveraging low-precision arithmetic. For problems with millions of degrees of freedom and thousands of eigenvalues, R-ChFSI attains final residual norms in the range of 10^{-12} to 10^{-14} , even with FP32 and TF32 arithmetic, significantly outperforming standard ChFSI in similar settings. In generalized eigenproblems, where approximate inverses are used, R-ChFSI achieves residual tolerances up to ten orders of magnitude lower, demonstrating its robustness to approximation errors. By efficiently utilizing modern hardware accelerators and reducing reliance on high-precision arithmetic, R-ChFSI provides a scalable and computationally efficient alternative for solving large-scale eigenproblems in high-performance computing environments.

1. Introduction

Eigenvalue problems arise in a wide range of disciplines, including science and engineering. In quantum systems, eigenproblems play a crucial role in quantum systems [1], with eigenvalues determining the energy

Email address: phanim@iisc.ac.in (Phani Motamarri*)

levels of the quantum systems, and in mechanical systems, eigenpairs relate to natural frequencies or buckling loads and mode shapes of structures [2, 3]. In control systems, the eigenvalues of the system matrix indicate stability and system response [4], while in fluid dynamics, they help determine the stability of fluid flows [5]. In acoustics, eigenproblems play an important role in wave propagation studies [6], and in chemistry and materials science, they determine vibrational modes of molecules [7], electronic energy levels [8] through the Hamiltonian eigenvalues. In the domains of computer science, machine learning and data science, eigenproblems arise in principal component analysis used for dimensionality reduction [9], in graph theory and network analysis through spectral clustering and graph partitioning algorithms [10], and in Markov Chains and PageRank algorithms [11], which rely on eigenvalues to model stochastic processes and to assess the importance of web pages. Efficient solution strategies to solve eigenproblems arising in different domains of science and engineering, particularly for large-scale problems, are of paramount importance and have been a subject of ongoing research in this era of heterogeneous computing.

Many scientific and engineering problems require solving large sparse matrix eigenproblems, where the goal is to compute only a small subset of the extreme eigenpairs, typically less than 0.5% of the matrix size. Specific applications include the discretization of partial differential equations using localized basis or grid-based methods and applications in graph theory and network analysis. The solution strategies for such eigenproblems often rely on fully iterative methods and are usually based on iterative orthogonal projection approaches. In these approaches, the large sparse matrix is orthogonally projected onto a carefully constructed smaller subspace rich in the wanted eigenvectors, followed by subspace diagonalization of the projected matrix and a subspace rotation step to recover the eigenvector estimates of the original sparse matrix. Popular iterative approaches include Davidson [12, 13], Generalized-Davidson [14], Jacobi-Davidson [15], Chebyshev-filtered subspace iteration (ChFSI) approach [16], LOBPCG [17], and PPCG [18]. Another key class of iterative techniques is based on Krylov subspace methods, namely the Arnoldi method [19], Lanczos methods [20] and their important variants, including implicit restart Arnoldi methods [21], Krylov-Schur method [22] and block-Krylov methods [23]. Our focus in this work involves the solution of large, sparse Hermitian eigenproblems using the ChFSI approach.

An important class of eigenproblems involves evolving matrices where the eigenspace of a large sparse matrix pencil must be computed repeatedly. These problems arise in electronic structure calculations using density functional theory [24], where a nonlinear eigenvalue problem is solved through a sequence of linear eigenvalue problems in a self-consistent fashion. Other examples of evolving matrices include subspace tracking in signal processing applications [25–27] and matrix completion problems [28] arising in multitask learning and recommender systems. A key feature of these problems is that they require computing an invariant subspace rather than individual eigenpairs. Subspace iteration methods [23, 29], which generalize single-vector power iteration, are particularly well suited for these problems because they allow efficient reuse of previously computed eigenspaces. This advantage makes these methods preferable to Krylov

subspace methods, which do not naturally accommodate evolving eigensubspaces. Approaches based on Chebyshev filtered subspace iteration (ChFSI) have become quite popular recently to solve both standard and generalized eigenproblems [30–33]. Although variants of ChFSI approaches combined with the Davidson method [34–37] have been proposed, the ChFSI approach remains the preferred choice in electronic structure codes based on density functional theory for solving the underlying nonlinear eigenvalue problem [38–41] due to its scalability and computational efficiency [42, 43]. Additionally, ChFSI is memory efficient compared to Davidson-type approaches and further offers an attractive alternative to preconditioned-type conjugate gradient approaches for problems, especially for problems where good preconditioners are unavailable.

Chebyshev filtered subspace iteration (ChFSI) belongs to a class of iterative orthogonal projection methods and relies on a Chebyshev filtering procedure that constructs a subspace rich in the desired eigenvectors exploiting the fast growth property of Chebyshev polynomials outside the interval $[-1,1]$, followed by a Rayleigh-Ritz step. Current work fills an important gap in the ChFSI approach by developing a residual-based approach to ChFSI that is tolerant to inexact matrix-vector products during the subspace construction step. Most importantly, we demonstrate that this approach is naturally amenable to the use of inexpensive matrix inverses while employing the ChFSI method to solve large sparse matrix generalized eigenproblems without affecting the convergence behavior. We also show that such an approach can be robust while leveraging low-precision matrix-vector products. Such capabilities are particularly relevant given the recent modifications in today’s heterogeneous computing architectures.

Modern hardware architectures have undergone substantial modifications in recent years due to the computational requirements of machine learning (ML) and artificial intelligence (AI) training. Owing to their high computational demands, these domains have necessitated the utilization of low-precision arithmetic. In response to this demand, hardware manufacturers have been enhancing support for low-precision floating-point formats, such as `tensorfloat32` and `bfloat16`, enabling significantly faster throughput and substantial performance improvements. Recent GPU architectures exemplify this shift towards reduced-precision arithmetic. Compared to the previous Hopper architecture, NVIDIA’s Blackwell GPUs, designed for AI/ML applications, demonstrate a notable decrease in peak double-precision (FP64) floating-point performance [44]. These architectural changes underscore the necessity to modify scientific computing algorithms to efficiently utilize low-precision processes without compromising accuracy [45, 46]. A significant amount of work has been done in recent years on mixed-precision algorithms for solving linear systems of equations [47–53] using the ideas of mixed precision preconditioning and iterative refinement. Such iterative refinement ideas have also been extended to sparse eigensolvers [48, 50], but they are inefficient when we require multiple eigenpairs. For this case, the ideas of mixed precision preconditioning for the LOBPCG eigensolver [54] and mixed precision orthogonalization and Rayleigh-Ritz have been explored for the LOBPCG and Chebyshev Filtered Subspace Iteration eigensolvers [38, 54, 55]. We note that in these works the evaluation of matrix-vector products still need to be performed in the higher precision arithmetic. We further note that the capacity

to accommodate inexact matrix-vector products facilitated by low-precision arithmetic can yield substantial performance enhancements. Algorithms that can accommodate inexact matrix-vector products while ensuring that errors remain within acceptable tolerances can efficiently utilize the capabilities of modern hardware, thereby reducing computational costs. The development of such algorithms becomes particularly important in light of the evolving hardware landscape.

In this work, we introduce a residual-based reformulation of the Chebyshev filtered subspace iteration (ChFSI) method [16, 31, 40, 56], referred to as the R-ChFSI method, for solving large-scale sparse Hermitian eigenvalue problems. The key novelty of R-ChFSI lies in its ability to accommodate inexact matrix-vector products while preserving convergence properties. This ability makes the proposed method particularly relevant for modern hardware architectures that favor low-precision arithmetic, significantly improving computational efficiency. The proposed R-ChFSI method is also well-suited for generalized eigenvalue problems, as it can employ approximate matrix inversion and avoid expensive matrix factorizations and iterative solvers that are otherwise typically required for such problems [33]. The core of our approach is a reformulated recurrence relation that modifies the standard ChFSI update step to operate on residuals rather than the guess of the eigenvectors. We then provide a mathematical justification demonstrating that this reformulation reduces the numerical error in the Chebyshev filtered subspace construction while employing inexact matrix-vector products compared to the traditional ChFSI recurrence relation. Our analysis establishes that the proposed R-ChFSI method effectively controls error propagation in the Chebyshev filtering process, leading to faster and more reliable convergence.

Through extensive benchmarking, we observe that R-ChFSI achieves comparable or superior residual tolerances while maintaining computational efficiency. Specifically, for benchmark systems with up to 7.6 million degrees of freedom (DoFs) and 14,000 wanted eigenvalues, the FP32 and TF32 variants of R-ChFSI achieve final residual norms within 10^{-12} to 10^{-14} , whereas standard ChFSI with the same precision fails to converge below 10^{-6} . Additionally, in generalized eigenvalue problems, where we employ a diagonal approximation to the matrix inverse, R-ChFSI attains a residual tolerance 10 orders of magnitude lower than standard ChFSI, demonstrating superior robustness to approximation errors. The improved convergence for generalized eigenvalue problems is particularly noteworthy, as it highlights the ability of R-ChFSI to handle approximate inverses while maintaining accuracy. In contrast, standard ChFSI is more sensitive to such approximations, often leading to a loss in accuracy or requiring significantly higher computational costs to achieve similar residual tolerances. This advantage of R-ChFSI is especially relevant in quantum chemistry and electronic structure calculations, where generalized eigenvalue problems frequently arise, and high computational costs constitute a significant bottleneck. By reducing dependence on exact matrix factorizations and high-precision arithmetic, R-ChFSI enables efficient exploitation of modern hardware accelerators, making large-scale eigenvalue computations more feasible in high-performance computing environments.

2. Mathematical Background

The Chebyshev filtered subspace iteration (ChFSI) [16, 23, 31, 40, 56] approach for solving the desired eigenpairs belongs to the category of iterative orthogonal projection methods and is one of the widely used strategies to compute the smallest n eigenvalues and their corresponding eigenvectors of large sparse matrices [33, 38, 39, 55, 57–65]. To describe the proposed eigensolver strategy based on the ChFSI approach, in the current work, we consider the Hermitian generalized eigenvalue problem of the form

$$\mathbf{A}\mathbf{u}_i = \lambda_i\mathbf{B}\mathbf{u}_i \text{ where } \mathbf{A} \in \mathbb{C}^{m \times m}, \mathbf{B} \in \mathbb{C}^{m \times m}. \quad (1)$$

where \mathbf{A} and \mathbf{B} are Hermitian matrices with \mathbf{B} being a positive-definite matrix. In addition, $\lambda_i \in \mathbb{R}$ and $\mathbf{u}_i \in \mathbb{C}^m : \forall i = 1, \dots, n$ denote the eigenvalue-eigenvector pairs corresponding to the smallest n eigenvalues. Equation (1) reduces to a standard eigenvalue problem when $\mathbf{B} = \mathbf{I}$ with \mathbf{I} denoting the $m \times m$ identity matrix. Without loss of generality, we assume that the eigenvalues are ordered as $\lambda_1 \leq \lambda_2 \leq \dots \leq \lambda_n \leq \lambda_{n+1} \leq \dots \leq \lambda_m$. For completeness and to introduce notations, we now provide a brief overview of the ChFSI algorithm, traditionally used to solve the eigenvalue problem corresponding to Eq. (1).

2.1. Chebyshev filtered subspace iteration and convergence properties

ChFSI leverages the properties of Chebyshev polynomials to efficiently filter out the components of the unwanted eigenvectors (corresponding to the remaining $m - n$ largest eigenvalues), thus enriching the trial subspace with the desired eigenvectors. To this end, we define the Chebyshev polynomial of degree k as

$$T_k(x) = \begin{cases} \cos(k \cos^{-1}(x)) & |x| \leq 1 \\ \cosh(k \cosh^{-1}(x)) & x > 1 \\ (-1)^k \cosh(k \cosh^{-1}(-x)) & x < -1 \end{cases} \quad (2)$$

and note that these polynomials exhibit the fastest growth in their magnitude when $|x| > 1$ while remaining bounded between $[-1, 1]$ when $|x| \leq 1$. To exploit this fast growth property of $T_k(x)$, an affine transformation that maps the largest $m - n$ eigenvalues to $[-1, 1]$ is defined, and consequently, the desired smallest n eigenvalues get mapped to values lying in $(-\infty, -1]$. To this end, we define the center of the unwanted spectrum as $c = (\lambda_{n+1} + \lambda_m)/2$ and the half-width of the unwanted spectrum as $e = (\lambda_{n+1} - \lambda_m)/2$ and hence the required affine transformation can now be represented as $\mathcal{L}(x) = (x - c)/e$. Standard implementations of ChFSI also scale the Chebyshev polynomials to prevent overflow [16, 23, 31, 40, 56] and consequently the scaled and shifted Chebyshev polynomials are defined as $C_k(x) = T_k(\mathcal{L}(x))/T_k(\mathcal{L}(a_{low}))$ where $a_{low} \leq \lambda_1$. We note that the ChFSI procedure for solving the eigenproblem in Eq. (1) is usually devised with the matrix $\mathbf{H} = \mathbf{B}^{-1}\mathbf{A}$ that has the same eigenpairs as $\mathbf{A}\mathbf{u}_j = \lambda_j\mathbf{B}\mathbf{u}_j$. This procedure for computing the smallest eigenpairs of Eq. (1) up to a specified tolerance τ on the eigenproblem residual norm, is summarized in Algorithm 1.

Algorithm 1: Subspace Iteration accelerated using Chebyshev polynomial of degree p (ChFSI)

1 *Initial Guess:* Let $\mathbf{X}^{(0)} = [\mathbf{x}_1^{(0)} \quad \mathbf{x}_2^{(0)} \quad \dots \quad \mathbf{x}_n^{(0)}]$ be the initial guess of the eigenvectors ($\{\mathbf{u}_j\}$).

while $r_j^{(i+1)} = \|\mathbf{A}\mathbf{x}_j^{(i+1)} - \epsilon_j^{(i+1)}\mathbf{B}\mathbf{x}_j^{(i+1)}\| \geq \tau$ **do**

2 *Chebyshev Filtered Subspace Construction:* In the i^{th} iteration, a Chebyshev filtered subspace

$\mathbf{Y}_p^{(i)}$ is constructed from the starting subspace $\mathbf{X}^{(i)}$ by evaluating $\mathbf{Y}_p^{(i)} = C_p(\mathbf{H})\mathbf{X}^{(i)}$ where p denotes the Chebyshev polynomial degree used. The construction of the filtered subspace is accomplished using the two-term recurrence relation for the Chebyshev polynomials i.e.,

$T_{k+1}(x) = 2xT_k(x) - T_{k-1}(x)$. Consequently, we define $\mathbf{Y}_k^{(i)} = C_k(\mathbf{H})\mathbf{X}^{(i)}$ for $k = 0, 1, \dots, p$ and thereby the two-term recurrence relation is written as:

$$\mathbf{Y}_{k+1}^{(i)} = \frac{2\sigma_{k+1}}{e}\mathbf{H}\mathbf{Y}_k^{(i)} - \frac{2\sigma_{k+1}c}{e}\mathbf{Y}_k^{(i)} - \sigma_k\sigma_{k+1}\mathbf{Y}_{k-1}^{(i)} \quad (3)$$

where $\mathbf{Y}_0^{(i)} = \mathbf{X}^{(i)}$ and $\mathbf{Y}_1^{(i)} = \frac{\sigma_1}{e}(\mathbf{H} - c\mathbf{I})\mathbf{X}^{(i)}$ and the coefficients are described by the recurrence relation $\sigma_{k+1} = 1 / \left(\sigma_k - \frac{2}{\sigma_1}\right)$ with $\sigma_1 = e / (a_{low} - c)$;

3 *Rayleigh-Ritz step:* Imposing the Galerkin orthogonality condition, we have the smaller $n \times n$ dense generalized eigenvalue problem, $\mathbf{Y}_p^{(i)\dagger} \mathbf{A} \mathbf{Y}_p^{(i)} \mathbf{E} = \mathbf{Y}_p^{(i)\dagger} \mathbf{B} \mathbf{Y}_p^{(i)} \mathbf{E} \mathbf{\Lambda}$, to be solved, where \mathbf{E} is the eigenvector matrix and $\mathbf{\Lambda}$ is the $n \times n$ diagonal matrix with the eigenvalues $\{\epsilon_j^{(i+1)}\}_{j=1}^n$ as its diagonal entries. The Ritz vectors are now given by $\mathbf{X}^{(i+1)} = \mathbf{Y}_p^{(i)} \mathbf{E}$;

2.1.1. Convergence analysis of ChFSI

To ensure completeness, we now provide a mathematical justification for the convergence of ChFSI. Note that $\|\cdot\|$ implies the 2-norm for vectors and vector-induced matrix 2-norm for matrices (spectral norm) throughout this work. In order to analyze convergence, we first define the maximum principal angle between two subspaces [66–68].

Definition 2.1. Let $\mathcal{X} \subset \mathbb{C}^{m \times m}$ and $\mathcal{Y} \subset \mathbb{C}^{m \times m}$ be subspaces of dimension n . The maximum principal angle between the two subspaces denoted by $\angle(\mathcal{X}, \mathcal{Y})$ is defined as

$$\sin \angle(\mathcal{X}, \mathcal{Y}) = \|\mathbf{X}_\perp^\dagger \mathbf{Y}\| = \|\mathbf{Y}_\perp^\dagger \mathbf{X}\|$$

where $\mathbf{X} \in \mathbb{C}^{m \times n}$ and $\mathbf{Y} \in \mathbb{C}^{m \times n}$ are matrices whose columns form an orthonormal basis for \mathcal{X} and \mathcal{Y} respectively. $\mathbf{X}_\perp \in \mathbb{C}^{m \times (m-n)}$ and $\mathbf{Y}_\perp \in \mathbb{C}^{m \times (m-n)}$ are matrices whose columns form an orthonormal basis spanning the orthogonal complements of \mathcal{X} and \mathcal{Y} respectively.

We also state a few results useful for further analysis

Lemma 2.1. Let the matrices $\mathbf{E} \in \mathbb{C}^{m \times n}$ and $\mathbf{E}_\perp \in \mathbb{C}^{m \times (m-n)}$ be given by $\mathbf{E} = \begin{bmatrix} \mathbf{I}_n \\ 0 \end{bmatrix}$ and $\mathbf{E}_\perp = \begin{bmatrix} 0 \\ \mathbf{I}_{m-n} \end{bmatrix}$

where \mathbf{I}_n and \mathbf{I}_{m-n} are the $n \times n$ and $(m-n) \times (m-n)$ identity matrices respectively. Let $\mathcal{E} = \mathcal{R}(\mathbf{E})$ and $\mathcal{E}_\perp = \mathcal{R}(\mathbf{E}_\perp)$ where $\mathcal{R}(\cdot)$ denotes range of a matrix. Then for any matrix $\mathbf{X} \in \mathbb{C}^{m \times n}$ with $\mathcal{X} = \mathcal{R}(\mathbf{X})$ satisfying $\mathcal{E}_\perp \cap \mathcal{X} = \{0\}$ or equivalently $\text{rank}(\mathbf{E}^\dagger \mathbf{X}) = n$, we have

$$\tan \angle(\mathcal{X}, \mathcal{E}) = \|\mathbf{E}_\perp^\dagger \mathbf{X} (\mathbf{E}^\dagger \mathbf{X})^{-1}\|$$

Proof. For a proof this statement we refer the reader to Zhu and Knyazev [67], Watkins [68]. \square

For the sake of convenience in the subsequent convergence analysis, we define the Hermitian matrix $\hat{\mathbf{H}} = \mathbf{B}^{-\frac{1}{2}} \mathbf{A} \mathbf{B}^{-\frac{1}{2}}$ allowing us to rewrite the generalized eigenproblem $\mathbf{A} \mathbf{U} = \mathbf{B} \mathbf{U} \mathbf{\Lambda}$, as a Hermitian standard eigenvalue problem $\hat{\mathbf{H}} \hat{\mathbf{U}} = \hat{\mathbf{U}} \mathbf{\Lambda}$, where $\hat{\mathbf{U}} = \mathbf{B}^{\frac{1}{2}} \mathbf{U}$ denotes the $m \times m$ unitary matrix with columns as eigenvectors of $\hat{\mathbf{H}}$ and $\mathbf{\Lambda}$ denotes the diagonal matrix comprising eigenvalues of $\hat{\mathbf{H}}$. Consider the partitioning of $\hat{\mathbf{U}}$ as $\begin{bmatrix} \hat{\mathbf{U}}_1 & \hat{\mathbf{U}}_2 \end{bmatrix}$ where $\hat{\mathbf{U}}_1$ is the $m \times n$ matrix whose columns are the eigenvectors corresponding to the lowest n eigenvalues and $\hat{\mathbf{U}}_2$ is the $m \times (m-n)$ matrix whose columns are the rest of the eigenvectors. We define the wanted eigenspace corresponding to the n smallest eigenvectors of $\hat{\mathbf{H}}$ as $\mathcal{S} = \mathcal{R}(\hat{\mathbf{U}}_1)$ and the unwanted eigenspace as $\mathcal{S}_\perp = \mathcal{R}(\hat{\mathbf{U}}_2)$. The trial subspace corresponding to $\hat{\mathbf{H}}$ at the beginning of i^{th} iteration is denoted as $\mathcal{S}^{(i)} = \mathcal{R}(\hat{\mathbf{X}}^{(i)})$ where $\hat{\mathbf{X}}^{(i)} = \mathbf{B}^{\frac{1}{2}} \mathbf{X}^{(i)}$. Further, the filtered subspace obtained at the end of this i^{th} iteration is denoted as $\mathcal{S}^{(i+1)} = \mathcal{R}(\hat{\mathbf{Y}}_p^{(i)})$ where $\hat{\mathbf{Y}}_p^{(i)} = \mathbf{B}^{\frac{1}{2}} \mathbf{Y}_p^{(i)}$. We note that using the relation $\mathbf{B}^{\frac{1}{2}} C_p(\mathbf{H}) \mathbf{B}^{-\frac{1}{2}} = C_p(\hat{\mathbf{H}})$ and $\mathbf{Y}_p^{(i)} = C_p(\mathbf{H}) \mathbf{X}^{(i)}$ from Algorithm 1, we can conclude that $\hat{\mathbf{Y}}_p^{(i)} = C_p(\hat{\mathbf{H}}) \hat{\mathbf{X}}^{(i)}$, i.e., $\mathcal{S}^{(i+1)} = C_p(\hat{\mathbf{H}}) \mathcal{S}^{(i)}$.

Theorem 2.1. For an n -dimensional space $\mathcal{S}^{(i)}$ satisfying $\mathcal{S}^{(i)} \cap \mathcal{S}_\perp = \{0\}$ where \mathcal{S}_\perp is the orthogonal complement of \mathcal{S} and $\mathcal{S}^{(i+1)} = C_p(\hat{\mathbf{H}}) \mathcal{S}^{(i)}$, we have the following inequality

$$\tan \angle(\mathcal{S}^{(i+1)}, \mathcal{S}) \leq \left| \frac{C_p(\lambda_{n+1})}{C_p(\lambda_n)} \right| \tan \angle(\mathcal{S}^{(i)}, \mathcal{S})$$

Proof. Since the maximum principal angle given by Definition 2.1 is invariant under unitary transformations, the tangent of the angles between the subspaces satisfy both $\tan \angle(\mathcal{S}^{(i+1)}, \mathcal{S}) = \tan \angle(\hat{\mathbf{U}}^\dagger \mathcal{S}^{(i+1)}, \hat{\mathbf{U}}^\dagger \mathcal{S})$ and $\tan \angle(\mathcal{S}^{(i)}, \mathcal{S}) = \tan \angle(\hat{\mathbf{U}}^\dagger \mathcal{S}^{(i)}, \hat{\mathbf{U}}^\dagger \mathcal{S})$. Since the space defined by $\hat{\mathbf{U}}^\dagger \mathcal{S}$ is the column space \mathcal{E} of the matrix $\mathbf{E} = \begin{bmatrix} \mathbf{I}_n \\ 0 \end{bmatrix}$, we have the above angles between subspaces satisfying $\tan \angle(\mathcal{S}^{(i+1)}, \mathcal{S}) = \tan \angle(\hat{\mathbf{U}}^\dagger \mathcal{S}^{(i+1)}, \mathcal{E})$

and $\tan \angle(\mathcal{S}^{(i)}, \mathcal{S}) = \tan \angle(\hat{\mathbf{U}}^\dagger \mathcal{S}^{(i)}, \mathcal{E})$. Consider a partitioning of the matrix $\hat{\mathbf{U}}^\dagger \hat{\mathbf{X}}^{(i)}$ as $\hat{\mathbf{U}}^\dagger \hat{\mathbf{X}}^{(i)} = \begin{bmatrix} \hat{\mathbf{Z}}_1^{(i)} \\ \hat{\mathbf{Z}}_2^{(i)} \end{bmatrix}$ where $\hat{\mathbf{Z}}_1^{(i)} = \hat{\mathbf{U}}_1^\dagger \hat{\mathbf{X}}^{(i)}$ and $\hat{\mathbf{Z}}_2^{(i)} = \hat{\mathbf{U}}_2^\dagger \hat{\mathbf{X}}^{(i)}$. We note that the assumption $\mathcal{S}^{(i)} \cap \mathcal{S}_\perp = \{0\}$ ensures that $\hat{\mathbf{Z}}_1^{(i)}$ is invertible, and consequently, we can write

$$\hat{\mathbf{U}}^\dagger \mathcal{S}^{(i)} = \mathcal{R}(\hat{\mathbf{U}}^\dagger \hat{\mathbf{X}}^{(i)}) = \mathcal{R} \left(\begin{bmatrix} \hat{\mathbf{Z}}_1^{(i)} \\ \hat{\mathbf{Z}}_2^{(i)} \end{bmatrix} \right)$$

Subsequently from Lemma 2.1 we have $\tan \angle(\mathcal{S}^{(i)}, \mathcal{S}) = \|\hat{\mathbf{Z}}_2^{(i)} \hat{\mathbf{Z}}_1^{(i)-1}\|$. Further, partitioning the diagonal matrix of eigenvalues $\mathbf{\Lambda}$, we have $\mathbf{\Lambda} = \begin{bmatrix} \mathbf{\Lambda}_1 & 0 \\ 0 & \mathbf{\Lambda}_2 \end{bmatrix}$ where $\mathbf{\Lambda}_1$ is the $n \times n$ diagonal matrix comprising of the wanted eigenvalues and $\mathbf{\Lambda}_2$ is the $(m-n) \times (m-n)$ diagonal matrix comprising of the unwanted eigenvalues. We can now write

$$\hat{\mathbf{U}}^\dagger \mathcal{S}^{(i+1)} = \hat{\mathbf{U}}^\dagger C_p(\hat{\mathbf{H}}) \hat{\mathbf{U}} \hat{\mathbf{U}}^\dagger \mathcal{S}^{(i)} = C_p(\mathbf{\Lambda}) \hat{\mathbf{U}}^\dagger \mathcal{S}^{(i)} = \mathcal{R} \left(\begin{bmatrix} C_p(\mathbf{\Lambda}_1) & 0 \\ 0 & C_p(\mathbf{\Lambda}_2) \end{bmatrix} \begin{bmatrix} \hat{\mathbf{Z}}_1^{(i)} \\ \hat{\mathbf{Z}}_2^{(i)} \end{bmatrix} \right) = \mathcal{R} \left(\begin{bmatrix} C_p(\mathbf{\Lambda}_1) \hat{\mathbf{Z}}_1^{(i)} \\ C_p(\mathbf{\Lambda}_2) \hat{\mathbf{Z}}_2^{(i)} \end{bmatrix} \right)$$

Consequently from Lemma 2.1 we have $\tan \angle(\mathcal{S}^{(i+1)}, \mathcal{S}) = \|C_p(\mathbf{\Lambda}_2) \hat{\mathbf{Z}}_2^{(i)} \hat{\mathbf{Z}}_1^{(i)-1} C_p(\mathbf{\Lambda}_1)^{-1}\|$ allowing us to write

$$\tan \angle(\mathcal{S}^{(i+1)}, \mathcal{S}) \leq \|C_p(\mathbf{\Lambda}_2)\| \|\hat{\mathbf{Z}}_2^{(i)} \hat{\mathbf{Z}}_1^{(i)-1}\| \|C_p(\mathbf{\Lambda}_1)^{-1}\| = \left| \frac{C_p(\lambda_{n+1})}{C_p(\lambda_n)} \right| \tan \angle(\mathcal{S}^{(i)}, \mathcal{S})$$

□

3. Approximation Methods for Chebyshev Filtered Subspace Construction

We note that the computationally dominant step in Chebyshev filtered subspace construction is the evaluation of the sparse-matrix multi-vector product $\mathbf{H}\mathbf{Y}_k^{(i)}$ in Eq. (3). A straightforward way to accelerate this step is to use approximations in the computation of $\mathbf{H}\mathbf{Y}_k^{(i)}$, allowing for improved efficiency. This should, in principle, allow for the use of various efficient approximate matrix multiplication techniques, including but not limited to mixed-precision arithmetic. However, we note that this requires an understanding of the convergence properties of ChFSI when such approximations are employed. We now adapt Theorem 2.1 for the case where approximations are used in computing $\mathbf{H}\mathbf{Y}_k^{(i)}$.

3.1. Convergence of ChFSI with inexact subspace construction

We now define $\underline{\mathcal{S}}^{(i+1)}$ as the space spanned by the columns of $\hat{\mathbf{Y}}_p^{(i)} = \mathbf{B}^{\frac{1}{2}} \mathbf{Y}_p^{(i)}$ with $\mathbf{Y}_p^{(i)}$ defined as $\mathbf{Y}_p^{(i)} = \underline{C_p(\mathbf{H})\mathbf{X}^{(i)}}$ where underline here denotes that approximations are introduced during matrix multiplications in Step 2 of Algorithm 1. We note that the columns of $\hat{\mathbf{X}}^{(i)} = \mathbf{B}^{\frac{1}{2}} \mathbf{X}^{(i)}$ form an orthonormal basis for $\mathcal{S}^{(i)}$.

Theorem 3.1. *For an n -dimensional space $\mathcal{S}^{(i)}$ satisfying $\mathcal{S}^{(i)} \cap \mathcal{S}_\perp = \{0\}$ and $\underline{\mathcal{S}}^{(i+1)} = \mathcal{R}(\underline{C_p(\mathbf{H})\mathbf{X}^{(i)}})$ we can write*

$$\tan \angle(\underline{\mathcal{S}}^{(i+1)}, \mathcal{S}) \leq \left(\frac{|C_p(\lambda_{n+1})| + \|\hat{\mathbf{\Delta}}_p^{(i)}\| \csc \angle(\mathcal{S}^{(i)}, \mathcal{S})}{|C_p(\lambda_n)| - \|\hat{\mathbf{\Delta}}_p^{(i)}\| \sec \angle(\mathcal{S}^{(i)}, \mathcal{S})} \right) \tan \angle(\mathcal{S}^{(i)}, \mathcal{S}) \quad (4)$$

where $\hat{\mathbf{\Delta}}_p^{(i)} = \underline{C_p(\hat{\mathbf{H}})\hat{\mathbf{X}}^{(i)}} - C_p(\hat{\mathbf{H}})\hat{\mathbf{X}}^{(i)}$

Proof. Partitioning the matrix $\hat{\mathbf{U}}^\dagger \hat{\mathbf{X}}^{(i)}$, we have $\hat{\mathbf{U}}^\dagger \hat{\mathbf{X}}^{(i)} = \begin{bmatrix} \hat{\mathbf{Z}}_1^{(i)} \\ \hat{\mathbf{Z}}_2^{(i)} \end{bmatrix}$ where $\hat{\mathbf{Z}}_1^{(i)} = \hat{\mathbf{U}}_1^\dagger \hat{\mathbf{X}}^{(i)}$ and $\hat{\mathbf{Z}}_2^{(i)} = \hat{\mathbf{U}}_2^\dagger \hat{\mathbf{X}}^{(i)}$.

We note that the assumption $\mathcal{S}^{(i)} \cap \mathcal{S}_\perp = \{0\}$ ensures that $\hat{\mathbf{Z}}_1^{(i)}$ is invertible. Consequently, we can write

$$\begin{aligned} \hat{\mathbf{U}}^\dagger \underline{\mathcal{S}}^{(i+1)} &= \mathcal{R} \left(\hat{\mathbf{U}}^\dagger C_p(\hat{\mathbf{H}}) \hat{\mathbf{X}}^{(i)} \right) = \mathcal{R} \left(\hat{\mathbf{U}}^\dagger C_p(\hat{\mathbf{H}}) \hat{\mathbf{X}}^{(i)} + \hat{\mathbf{U}}^\dagger \hat{\Delta}_p^{(i)} \right) = \mathcal{R} \left(C_p(\mathbf{\Lambda}) \hat{\mathbf{U}}^\dagger \hat{\mathbf{X}}^{(i)} + \hat{\mathbf{U}}^\dagger \hat{\Delta}_p^{(i)} \right) \\ &= \mathcal{R} \left(\begin{bmatrix} C_p(\mathbf{\Lambda}_1) \hat{\mathbf{Z}}_1^{(i)} + \hat{\mathbf{U}}_1^\dagger \hat{\Delta}_p^{(i)} \\ C_p(\mathbf{\Lambda}_2) \hat{\mathbf{Z}}_2^{(i)} + \hat{\mathbf{U}}_2^\dagger \hat{\Delta}_p^{(i)} \end{bmatrix} \right) \end{aligned}$$

Consequently, from Lemma 2.1 we can write

$$\begin{aligned} \tan \angle(\underline{\mathcal{S}}^{(i+1)}, \mathcal{S}) &= \left\| \left(C_p(\mathbf{\Lambda}_2) \hat{\mathbf{Z}}_2^{(i)} + \hat{\mathbf{U}}_2^\dagger \hat{\Delta}_p^{(i)} \right) \left(C_p(\mathbf{\Lambda}_1) \hat{\mathbf{Z}}_1^{(i)} + \hat{\mathbf{U}}_1^\dagger \hat{\Delta}_p^{(i)} \right)^{-1} \right\| \\ &= \left\| \left(C_p(\mathbf{\Lambda}_2) \hat{\mathbf{Z}}_2^{(i)} \hat{\mathbf{Z}}_1^{(i)-1} C_p(\mathbf{\Lambda}_1)^{-1} + \hat{\mathbf{U}}_2^\dagger \hat{\Delta}_p^{(i)} \hat{\mathbf{Z}}_1^{(i)-1} C_p(\mathbf{\Lambda}_1)^{-1} \right) \left(\mathbf{I} + \hat{\mathbf{U}}_1^\dagger \hat{\Delta}_p^{(i)} \hat{\mathbf{Z}}_1^{(i)-1} C_p(\mathbf{\Lambda}_1)^{-1} \right)^{-1} \right\| \\ &\leq \frac{\|C_p(\mathbf{\Lambda}_2) \hat{\mathbf{Z}}_2^{(i)} \hat{\mathbf{Z}}_1^{(i)-1} C_p(\mathbf{\Lambda}_1)^{-1}\| + \|\hat{\Delta}_p^{(i)} \hat{\mathbf{Z}}_1^{(i)-1} C_p(\mathbf{\Lambda}_1)^{-1}\|}{1 - \|\hat{\Delta}_p^{(i)} \hat{\mathbf{Z}}_1^{(i)-1} C_p(\mathbf{\Lambda}_1)^{-1}\|} \end{aligned} \quad (5)$$

Note that in the last step, we have assumed that $\|\hat{\Delta}_p^{(i)} \hat{\mathbf{Z}}_1^{(i)-1} C_p(\mathbf{\Lambda}_1)^{-1}\| < 1$, and using the fact that $\|\hat{\mathbf{Z}}_1^{(i)-1}\| = \sec \angle(\mathcal{S}^{(i)}, \mathcal{S})$, a sufficient condition for this to be true is $|C_p(\lambda_n)| \cos \angle(\mathcal{S}^{(i)}, \mathcal{S}) > \|\hat{\Delta}_p^{(i)}\|$. Upon further simplification using sub-multiplicative property of matrix spectral norms and triangle inequality, the inequality in Eq. (5) can be written as

$$\begin{aligned} \tan \angle(\underline{\mathcal{S}}^{(i+1)}, \mathcal{S}) &\leq \frac{\|C_p(\mathbf{\Lambda}_2)\| \|\hat{\mathbf{Z}}_2^{(i)} \hat{\mathbf{Z}}_1^{(i)-1}\| \|C_p(\mathbf{\Lambda}_1)^{-1}\| + \|\hat{\Delta}_p^{(i)}\| \|\hat{\mathbf{Z}}_1^{(i)-1}\| \|C_p(\mathbf{\Lambda}_1)^{-1}\|}{1 - \|\hat{\Delta}_p^{(i)}\| \|\hat{\mathbf{Z}}_1^{(i)-1}\| \|C_p(\mathbf{\Lambda}_1)^{-1}\|} \\ &\leq \frac{|C_p(\lambda_{n+1})| \sin \angle(\mathcal{S}^{(i)}, \mathcal{S}) + \|\hat{\Delta}_p^{(i)}\|}{|C_p(\lambda_n)| \cos \angle(\mathcal{S}^{(i)}, \mathcal{S}) - \|\hat{\Delta}_p^{(i)}\|} \\ &= \left(\frac{|C_p(\lambda_{n+1})| + \|\hat{\Delta}_p^{(i)}\| \csc \angle(\mathcal{S}^{(i)}, \mathcal{S})}{|C_p(\lambda_n)| - \|\hat{\Delta}_p^{(i)}\| \sec \angle(\mathcal{S}^{(i)}, \mathcal{S})} \right) \tan \angle(\mathcal{S}^{(i)}, \mathcal{S}) \end{aligned}$$

which proves the desired inequality in the theorem. \square

Now for convergence we demand that $\angle(\underline{\mathcal{S}}^{(i+1)}, \mathcal{S}) < \angle(\mathcal{S}^{(i)}, \mathcal{S})$ and consequently we require

$$|C_p(\lambda_n)| - |C_p(\lambda_{n+1})| > \|\hat{\Delta}_p^{(i)}\| \left(\sec \angle(\mathcal{S}^{(i)}, \mathcal{S}) + \csc \angle(\mathcal{S}^{(i)}, \mathcal{S}) \right) \quad \forall i = 0, \dots, \infty \quad (6)$$

We note that if $\|\hat{\Delta}_p^{(i)}\|$ remains nearly constant with iteration i , the right-hand side of the inequality in Eq. (6) keeps increasing as we approach the exact eigenspace and beyond a certain angle $\angle(\mathcal{S}^{(i)}, \mathcal{S})$ this inequality gets violated. Consequently, the angle stops decreasing and we cannot approach the exact eigenspace beyond that point. To this end, for robust convergence, we require that $\|\hat{\Delta}_p^{(i)}\|$ also decreases as we approach the exact eigenspace, and we demonstrate that our proposed residual-based reformulation of

Chebyshev filtered subspace iteration procedure (R-ChFSI) algorithm described subsequently accomplishes this. We further note that $(\sec \angle(\mathcal{S}^{(i)}, \mathcal{S}) + \csc \angle(\mathcal{S}^{(i)}, \mathcal{S})) \geq 2\sqrt{2}$ and consequently for convergence on any approximation employed, we obtain the following necessary condition on $\|\hat{\Delta}_p^{(i)}\|$ from Eq. (6),

$$\|\hat{\Delta}_p^{(i)}\| < \frac{|C_p(\lambda_n)| - |C_p(\lambda_{n+1})|}{2\sqrt{2}}. \quad (7)$$

3.2. Standard Eigenvalue Problems

In this section we analyze the case of $\mathbf{B} = \mathbf{I}$ and consequently $\hat{\mathbf{H}} = \mathbf{B}^{-\frac{1}{2}}\mathbf{A}\mathbf{B}^{-\frac{1}{2}} = \mathbf{H} = \mathbf{A}$ is a Hermitian matrix. We now consider the specific case of utilizing a lower precision to compute the matrix product $\mathbf{H}\mathbf{Y}_k^{(i)}$ in the Chebyshev recurrence relation defined by Eq. (3). We first evaluate the upper bound on $\Delta_p^{(i)}$ if one naively replaces the matrix product $\mathbf{H}\mathbf{Y}_k^{(i)}$ in Eq. (3) with the approximate matrix product denoted as $\underline{\mathbf{H}}\mathbf{Y}_k^{(i)} = \mathbf{H} \otimes \mathbf{Y}_k^{(i)}$, where \otimes represents the product evaluated with lower precision arithmetic, and argue that this method will fail to converge to the same residual tolerance that can be achieved with full precision matrix products. We then propose a residual-based reformulation of the recurrence relation and argue that the proposed reformulation allows for convergence to similar residual tolerances that can be achieved with full precision matrix products.

3.2.1. Traditional Chebyshev filtering approach employing low-precision matrix-products

Employing low-precision matrix-products, the recurrence relation in Eq. (3) for $\underline{\mathbf{Y}}_k^{(i)} = C_k(\mathbf{H}) \otimes \mathbf{X}^{(i)}$, where $k = 2, \dots, p$ can be written as

$$\underline{\mathbf{Y}}_{k+1}^{(i)} = a_k \mathbf{H} \otimes \underline{\mathbf{Y}}_k^{(i)} + b_k \underline{\mathbf{Y}}_k^{(i)} + c_k \underline{\mathbf{Y}}_{k-1}^{(i)} \quad (8)$$

where for convenience of notation we have defined

$$a_k = \frac{2\sigma_{k+1}}{e} \quad b_k = -\frac{2\sigma_{k+1}c}{e} \quad c_k = -\sigma_k\sigma_{k+1}$$

and with the initial conditions $\underline{\mathbf{Y}}_0^{(i)} = \mathbf{X}^{(i)}$ and $\underline{\mathbf{Y}}_1^{(i)} = \frac{\sigma_1}{e}(\mathbf{H} - c\mathbf{I})\mathbf{X}^{(i)}$. This allows us to write a recurrence relation for $\Delta_k^{(i)} = \underline{\mathbf{Y}}_k^{(i)} - \mathbf{Y}_k^{(i)}$ as

$$\Delta_{k+1}^{(i)} = a_k \mathbf{H} \Delta_k^{(i)} + b_k \Delta_k^{(i)} + c_k \Delta_{k-1}^{(i)} + a_k (\mathbf{H} \otimes \underline{\mathbf{Y}}_k^{(i)} - \mathbf{H}\underline{\mathbf{Y}}_k^{(i)}) \quad (9)$$

with the initial conditions $\Delta_0^{(i)} = \Delta_1^{(i)} = 0$. We now state some useful results required for further analysis

Lemma 3.1. *If $\mathbf{H} \in \mathbb{C}^{m \times m}$ and $\mathbf{X} \in \mathbb{C}^{m \times n}$, the spectral norm of the error in evaluating the matrix product $\mathbf{H}\mathbf{X}$ due to floating point approximations satisfies $\|\mathbf{H}\mathbf{X} - \mathbf{H} \otimes \mathbf{X}\| \leq \gamma_m \|\mathbf{H}\| \|\mathbf{X}\|$*

Proof. This is a straightforward application of the results derived in [69, section 3.5]. We note that γ_m is a constant that depends on m , and the machine precision of the floating point arithmetic (denoted as ε_M). For the case of dense real matrices, we have $\gamma_m = m\varepsilon_M/(1 - m\varepsilon_M)$ and for dense complex matrices, it

needs to be appropriately modified as described in [69, section 3.6]. Further, we also note that in the case where \mathbf{H} is sparse, significantly tighter bounds independent of m can be achieved depending on the specific implementations of the sparse matrix-dense matrix multiplication routines. \square

Theorem 3.2. *The spectral norm of the error $\Delta_k^{(i)} = \mathbf{Y}_k^{(i)} - \mathbf{Y}_k^{(i)}$ in the subspace construction using lower precision arithmetic in matrix-products of the recurrence relation Eq. (3) satisfies $\|\Delta_k^{(i)}\| \leq \gamma_m \eta_k$ for $k = 0, 1, \dots, p$ where η_k is some finite constant that depends on k*

Proof. We argue by induction that $\|\Delta_k^{(i)}\| \leq \gamma_m \eta_k$ where η_k is some finite constant that depends on k . Recall from the initial conditions on Eq. (9), we have $\Delta_0^{(i)} = \Delta_1^{(i)} = 0$. Further, we assume the induction hypothesis for $k = r - 1$ and $k = r$ i.e., the inequalities $\|\Delta_{r-1}^{(i)}\| \leq \gamma_m \eta_{r-1}$ and $\|\Delta_r^{(i)}\| \leq \gamma_m \eta_r$ are true and now we need to show $\|\Delta_{r+1}^{(i)}\| \leq \gamma_m \eta_{r+1}$. Subsequently, from the induction hypothesis, we have the following expression for $\|\Delta_{r+1}^{(i)}\|$ using Eq. (9)

$$\|\Delta_{r+1}^{(i)}\| \leq |a_r| \|\mathbf{H}\| \eta_r \gamma_m + |b_r| \eta_r \gamma_m + |c_r| \eta_{r-1} \gamma_m + |a_r| \|\mathbf{H} \otimes \mathbf{Y}_r^{(i)} - \mathbf{H} \mathbf{Y}_r^{(i)}\| \quad (10)$$

$$\leq |a_r| \|\mathbf{H}\| \eta_r \gamma_m + |b_r| \eta_r \gamma_m + |c_r| \eta_{r-1} \gamma_m + |a_r| \|\mathbf{H}\| \|\mathbf{Y}_r^{(i)}\| \gamma_m \quad (11)$$

where we have used Lemma 3.1. We further note that $\|\mathbf{Y}_r^{(i)}\| = \|\Delta_r^{(i)} + \mathbf{Y}_r^{(i)}\| \leq \gamma_m \eta_r + \|\mathbf{Y}_r^{(i)}\| \leq \gamma_m \eta_r + \|C_r(\mathbf{H}) \mathbf{X}^{(i)}\| \leq \gamma_m \eta_r + \|C_r(\mathbf{H})\|$ and consequently we can write

$$\|\Delta_{r+1}^{(i)}\| \leq [|a_r| \|\mathbf{H}\| \eta_r + |b_r| \eta_r + |c_r| \eta_{r-1} + |a_r| \|\mathbf{H}\| (\gamma_m \eta_r + \|C_r(\mathbf{H})\|)] \gamma_m \quad (12)$$

Defining $\eta_{r+1} = |a_r| \|\mathbf{H}\| \eta_r + |b_r| \eta_r + |c_r| \eta_{r-1} + |a_r| \|\mathbf{H}\| (\gamma_m \eta_r + \|C_r(\mathbf{H})\|)$, we have $\|\Delta_{r+1}^{(i)}\| \leq \gamma_m \eta_{r+1}$ from Eq. (12). Hence using induction, we argue that $\|\Delta_k^{(i)}\| \leq \gamma_m \eta_k$ for $k = 0, 1, \dots, p$ \square

We now discuss the implications of the above Theorem 3.2 within the context of Eq. (6). Without loss of generality, we assume that our initial guess of trial subspace $\mathcal{S}^{(i)}$ at $i = 0$ satisfies the inequality below as stated in Eq. (6).

$$|C_p(\lambda_n)| - |C_p(\lambda_{n+1})| > \|\hat{\Delta}_p^{(i)}\| \left(\sec \angle(\mathcal{S}^{(i)}, \mathcal{S}) + \csc \angle(\mathcal{S}^{(i)}, \mathcal{S}) \right) \quad (13)$$

While the above inequality is satisfied, $\angle(\mathcal{S}^{(i)}, \mathcal{S})$ reduces as i increases (from Theorem 3.1). However, we note that the RHS of this equation does not monotonically decrease with a decrease in $\angle(\mathcal{S}^{(i)}, \mathcal{S})$ and increases as $\angle(\mathcal{S}^{(i)}, \mathcal{S})$ approaches 0. Thus, it stands to reason that beyond a certain value of $\angle(\mathcal{S}^{(i)}, \mathcal{S})$, the inequality in Eq. (13) no longer holds, and we cannot approach the wanted eigenspace beyond this point. Under the condition that $\gamma_m \eta_p \ll |C_p(\lambda_n)| - |C_p(\lambda_{n+1})|$, we can estimate the closest angle that can be achieved and is given by the following expression

$$\angle(\mathcal{S}^{(i)}, \mathcal{S}) \approx \frac{\gamma_m \eta_p}{|C_p(\lambda_n)| - |C_p(\lambda_{n+1})|} \quad (14)$$

We now propose a residual-based reformulation of ChFSI and argue that the proposed method does not suffer from this stagnation behavior even when employing lower precision arithmetic in matrix products.

3.2.2. Proposed residual-based Chebyshev filtering approach

We now propose a residual-based reformulation of the recurrence relation defined in Eq. (3). To this end we define the residual \mathbf{R}_k^i in a given iteration i for $k = 0, \dots, p$ in the following way:

$$\mathbf{R}_k^{(i)} = C_k(\mathbf{H})\mathbf{X}^{(i)} - \mathbf{X}^{(i)}C_k(\mathbf{\Lambda}^{(i)}) = \mathbf{Y}_k^{(i)} - \mathbf{X}^{(i)}\mathbf{\Lambda}_k^{(i)} \quad \text{for } k = 0, \dots, p \quad (15)$$

where we have defined $\mathbf{\Lambda}_k^{(i)} = C_k(\mathbf{\Lambda}^{(i)})$ and recall p is the maximum Chebyshev polynomial degree used in the subspace construction step.

Proposition 3.1. *The recurrence relation given by Eq. (3) can be reformulated in terms of the residuals defined by $\mathbf{R}_k^{(i)} = \mathbf{Y}_k^{(i)} - \mathbf{X}^{(i)}\mathbf{\Lambda}_k^{(i)}$ as*

$$\mathbf{R}_{k+1}^{(i)} = a_k \mathbf{H}\mathbf{R}_k^{(i)} + b_k \mathbf{R}_k^{(i)} + c_k \mathbf{R}_{k-1}^{(i)} + a_k \mathbf{R}^{(i)} \mathbf{\Lambda}_k^{(i)} \quad (16)$$

$$\mathbf{\Lambda}_{k+1}^{(i)} = a_k \mathbf{\Lambda}_k^{(i)} \mathbf{\Lambda}^{(i)} + b_k \mathbf{\Lambda}_k^{(i)} + c_k \mathbf{\Lambda}_{k-1}^{(i)} \quad (17)$$

where $\mathbf{R}_0^{(i)} = 0$ and $\mathbf{R}_1^{(i)} = \frac{\sigma_1}{e} \mathbf{R}^{(i)}$ with $\mathbf{R}^{(i)} = \mathbf{H}\mathbf{X}^{(i)} - \mathbf{X}^{(i)}\mathbf{\Lambda}^{(i)}$ and further we have $a_k = 2\sigma_{k+1}/e$, $b_k = -2\sigma_{k+1}c/e$, and $c_k = -\sigma_k\sigma_{k+1}$

Proof. The recurrence relation for $\mathbf{\Lambda}_k^{(i)} = C_k(\mathbf{\Lambda}^{(i)})$ can be written as

$$\mathbf{\Lambda}_{k+1}^{(i)} = a_k \mathbf{\Lambda}_k^{(i)} \mathbf{\Lambda}^{(i)} + b_k \mathbf{\Lambda}_k^{(i)} + c_k \mathbf{\Lambda}_{k-1}^{(i)}$$

Multiplying with $\mathbf{X}^{(i)}$ and subtracting from Eq. (3), we have

$$\mathbf{Y}_{k+1}^{(i)} - \mathbf{X}^{(i)}\mathbf{\Lambda}_{k+1}^{(i)} = a_k (\mathbf{H}\mathbf{Y}_k^{(i)} - \mathbf{X}^{(i)}\mathbf{\Lambda}_k^{(i)} \mathbf{\Lambda}^{(i)}) + b_k (\mathbf{Y}_k^{(i)} - \mathbf{X}^{(i)}\mathbf{\Lambda}_k^{(i)}) + c_k (\mathbf{Y}_{k-1}^{(i)} - \mathbf{X}^{(i)}\mathbf{\Lambda}_k^{(i)}) \quad (18)$$

$$\implies \mathbf{R}_{k+1}^{(i)} = a_k \mathbf{H}\mathbf{R}_k^{(i)} + b_k \mathbf{R}_k^{(i)} + c_k \mathbf{R}_{k-1}^{(i)} + a_k \mathbf{R}^{(i)} \mathbf{\Lambda}_k^{(i)} \quad (19)$$

□

After computing $\mathbf{R}_p^{(i)}$ using this recurrence relation we can now recover the desired subspace $\mathbf{Y}_p^{(i)}$ using the relation in Eq. (15) i.e., $\mathbf{Y}_p^{(i)} = \mathbf{R}_p^{(i)} + \mathbf{X}^{(i)}\mathbf{\Lambda}_p^{(i)}$. We note that using approximate matrix multiplication for evaluating $\mathbf{H}\mathbf{R}_k^{(i)}$ we can write the following recurrence relation

$$\underline{\mathbf{R}}_{k+1}^{(i)} = a_k \mathbf{H} \otimes \underline{\mathbf{R}}_k^{(i)} + b_k \underline{\mathbf{R}}_k^{(i)} + c_k \underline{\mathbf{R}}_{k-1}^{(i)} + a_k \mathbf{R}^{(i)} \mathbf{\Lambda}_k^{(i)} \quad (20)$$

and consequently, we have $\underline{\mathbf{Y}}_k^{(i)} = \underline{\mathbf{R}}_k^{(i)} + \mathbf{X}^{(i)}\mathbf{\Lambda}_k^{(i)}$. This allows us to write a recurrence relation for $\underline{\mathbf{\Delta}}_k^{(i)} = \underline{\mathbf{Y}}_k^{(i)} - \mathbf{Y}_k^{(i)} = \underline{\mathbf{R}}_k^{(i)} - \mathbf{R}_k^{(i)}$ as

$$\underline{\mathbf{\Delta}}_{k+1}^{(i)} = a_k \mathbf{H}\underline{\mathbf{\Delta}}_k^{(i)} + b_k \underline{\mathbf{\Delta}}_k^{(i)} + c_k \underline{\mathbf{\Delta}}_{k-1}^{(i)} + a_k (\mathbf{H} \otimes \underline{\mathbf{R}}_k^{(i)} - \mathbf{H}\mathbf{R}_k^{(i)}) \quad (21)$$

where $\underline{\mathbf{\Delta}}_0^{(i)} = \underline{\mathbf{\Delta}}_1^{(i)} = 0$. We now prove a result useful for further analysis

Lemma 3.2. *The spectral norm of the residual matrix defined by $\mathbf{R}_k^{(i)} = C_k(\mathbf{H})\mathbf{X}^{(i)} - \mathbf{X}^{(i)}C_k(\mathbf{\Lambda}^{(i)})$ for $k = 0, \dots, p$ is bounded by $\|\mathbf{R}_k^{(i)}\| \leq f_k \|\mathbf{R}^{(i)}\|$ where f_k is a finite constant and $\mathbf{R}^{(i)} = \mathbf{H}\mathbf{X}^{(i)} - \mathbf{X}^{(i)}\mathbf{\Lambda}^{(i)}$*

Proof. We define the polynomial $P_{k-1}(\mathbf{H}, \epsilon_j^{(i)})$ of degree $k-1$ obtained by the following factorization

$$C_k(\mathbf{H}) - C_k(\epsilon_j^{(i)}) = P_{k-1}(\mathbf{H}, \epsilon_j^{(i)})(\mathbf{H} - \epsilon_j^{(i)}\mathbf{I}) \quad (22)$$

Consequently the j -th column of $\mathbf{R}_k^{(i)}$ can then be written as

$$\left(C_k(\mathbf{H}) - C_k(\epsilon_j^{(i)})\right) \mathbf{x}_j = P_{k-1}(\mathbf{H}, \epsilon_j^{(i)})(\mathbf{H} - \epsilon_j^{(i)}\mathbf{I})\mathbf{x}_j = P_{k-1}(\mathbf{H}, \epsilon_j^{(i)})(\mathbf{H}\mathbf{x}_j - \epsilon_j^{(i)}\mathbf{x}_j) \quad (23)$$

where \mathbf{x}_j is the j -th column of $\mathbf{X}^{(i)}$ and $\epsilon_j^{(i)}$ is the j -th diagonal element of $\mathbf{\Lambda}^{(i)}$. Using the fact that spectral norm of a matrix is bounded by the matrix's Frobenius norm, we can write the following inequality using Eq. (23)

$$\|\mathbf{R}_k^{(i)}\|^2 \leq \sum_{j=1}^n \|P_{k-1}(\mathbf{H}, \epsilon_j^{(i)})(\mathbf{H}\mathbf{x}_j - \epsilon_j^{(i)}\mathbf{x}_j)\|^2 \quad (24)$$

Using the sub-multiplicative property of spectral norm, we have the following

$$\|P_k(\mathbf{H}, \epsilon_j^{(i)})(\mathbf{H}\mathbf{x}_j - \epsilon_j^{(i)}\mathbf{x}_j)\| \leq \|P_{k-1}(\mathbf{H}, \epsilon_j^{(i)})\| \|\mathbf{H}\mathbf{x}_j - \epsilon_j^{(i)}\mathbf{x}_j\| \quad (25)$$

and consequently, we can write

$$\|\mathbf{R}_k^{(i)}\|^2 \leq \left(\max_j \|P_{k-1}(\mathbf{H}, \epsilon_j^{(i)})\|\right)^2 \sum_{j=1}^n \|\mathbf{H}\mathbf{x}_j - \epsilon_j^{(i)}\mathbf{x}_j\|^2 \quad (26)$$

$$\implies \|\mathbf{R}_k^{(i)}\| \leq \left(\sqrt{n} \max_j \|P_{k-1}(\mathbf{H}, \epsilon_j^{(i)})\|\right) \|\mathbf{R}^{(i)}\| \quad (27)$$

where in the last step of the above inequality we have used the fact that Frobenius norm of a matrix is bounded by square root of the size of the matrix times the matrix's spectral norm. Now, defining $f_k = \sqrt{n} \max_j \|P_{k-1}(\mathbf{H}, \epsilon_j^{(i)})\|$, we have $\|\mathbf{R}_k^{(i)}\| \leq f_k \|\mathbf{R}^{(i)}\|$. \square

Lemma 3.3. *The spectral norm of the error $\mathbf{\Delta}_k^{(i)} = \underline{\mathbf{Y}}_k^{(i)} - \mathbf{Y}_k^{(i)}$ in the subspace construction using lower precision arithmetic in matrix-products of the recurrence relation Eq. (20) satisfies $\|\mathbf{\Delta}_k^{(i)}\| \leq \gamma_m \tilde{\eta}_k \|\mathbf{R}^{(i)}\|$ for $k = 0, 1, \dots, p$ where $\tilde{\eta}_k$ is some finite constant that depends on k .*

Proof. We argue by induction that $\|\mathbf{\Delta}_k^{(i)}\| \leq \gamma_m \tilde{\eta}_k \|\mathbf{R}^{(i)}\|$ where $\tilde{\eta}_k$ is some non-zero finite constant that depends on k . To this end, assuming the induction hypothesis for $k = r-1$ and $k = r$, we have $\|\mathbf{\Delta}_{r-1}^{(i)}\| \leq \gamma_m \tilde{\eta}_{r-1} \|\mathbf{R}^{(i)}\|$ and $\|\mathbf{\Delta}_r^{(i)}\| \leq \gamma_m \tilde{\eta}_r \|\mathbf{R}^{(i)}\|$. Subsequently, the following inequality is true for $\|\mathbf{\Delta}_{r+1}^{(i)}\|$ from Eq. (21)

$$\|\mathbf{\Delta}_{r+1}^{(i)}\| \leq |a_r| \|\mathbf{H}\| \tilde{\eta}_r \gamma_m \|\mathbf{R}^{(i)}\| + |b_r| \tilde{\eta}_r \gamma_m \|\mathbf{R}^{(i)}\| + |c_r| \tilde{\eta}_{r-1} \gamma_m \|\mathbf{R}^{(i)}\| + |a_r| \|\mathbf{H} \otimes \mathbf{R}_r^{(i)} - \mathbf{H}\mathbf{R}_r^{(i)}\| \quad (28)$$

$$\leq |a_r| \|\mathbf{H}\| \tilde{\eta}_r \gamma_m \|\mathbf{R}^{(i)}\| + |b_r| \tilde{\eta}_r \gamma_m \|\mathbf{R}^{(i)}\| + |c_r| \tilde{\eta}_{r-1} \gamma_m \|\mathbf{R}^{(i)}\| + |a_r| \|\mathbf{H}\| \|\mathbf{R}_r^{(i)}\| \gamma_m \quad (29)$$

where we have used Lemma 3.1. We further note that using Lemma 3.2 we can write $\|\underline{\mathbf{R}}_r^{(i)}\| = \|\underline{\Delta}_r^{(i)} + \mathbf{R}_r^{(i)}\| \leq \gamma_m \tilde{\eta}_r \|\mathbf{R}^{(i)}\| + \|\mathbf{R}_r^{(i)}\| \leq \gamma_m \tilde{\eta}_r \|\mathbf{R}^{(i)}\| + f_r \|\mathbf{R}^{(i)}\|$ and consequently we can write

$$\|\underline{\Delta}_{r+1}^{(i)}\| \leq \left[|a_r| \|\mathbf{H}\| \tilde{\eta}_r + |b_r| \tilde{\eta}_r + |c_r| \tilde{\eta}_{r-1} + |a_r| \|\mathbf{H}\| (\gamma_m \tilde{\eta}_r + f_r) \right] \gamma_m \|\mathbf{R}^{(i)}\| \quad (30)$$

Defining $\tilde{\eta}_{r+1} = |a_r| \|\mathbf{H}\| \tilde{\eta}_r + |b_r| \tilde{\eta}_r + |c_r| \tilde{\eta}_{r-1} + |a_r| \|\mathbf{H}\| (\gamma_m \tilde{\eta}_r + f_r)$ we have $\|\underline{\Delta}_{r+1}^{(i)}\| \leq \gamma_m \tilde{\eta}_{r+1} \|\mathbf{R}^{(i)}\|$. Hence using induction, we argue that $\|\underline{\Delta}_{k+1}^{(i)}\| \leq \gamma_m \tilde{\eta}_{k+1} \|\mathbf{R}^{(i)}\|$ for $k = 0, 1, \dots, p$ \square

Lemma 3.4. *The norm of the residual $\mathbf{R}^{(i)}$ is bounded by*

$$\|\mathbf{R}^{(i)}\| \leq 2\|\mathbf{H}\| \sin \angle(\mathcal{S}^{(i)}, \mathcal{S}) \quad (31)$$

Proof. We have, $\mathbf{R}^{(i)} = \mathbf{H}\mathbf{X}^{(i)} - \mathbf{X}^{(i)}\mathbf{\Lambda}^{(i)}$ and $\mathbf{\Lambda}^{(i)}$ can be written as $\mathbf{\Lambda}^{(i)} = \mathbf{X}^{(i)\dagger} \mathbf{H}\mathbf{X}^{(i)}$ allowing us to write $\mathbf{R}^{(i)} = (\mathbf{I} - \mathbf{X}^{(i)}\mathbf{X}^{(i)\dagger})\mathbf{H}\mathbf{X}^{(i)}$. Let $\hat{\mathbf{U}} = [\hat{\mathbf{u}}_1 \quad \hat{\mathbf{u}}_2 \quad \dots \quad \hat{\mathbf{u}}_m]$ be an $m \times m$ unitary matrix with the eigenvectors of \mathbf{H} as its columns and $\mathbf{\Lambda} = \hat{\mathbf{U}}^\dagger \hat{\mathbf{\Lambda}} \hat{\mathbf{U}}$ is the diagonal matrix of the eigenvalues. Consider a partitioning of $\hat{\mathbf{U}}$ as $[\hat{\mathbf{U}}_1 \quad \hat{\mathbf{U}}_2]$ where $\hat{\mathbf{U}}_1$ is the $m \times n$ matrix corresponding to the wanted eigenvectors and $\hat{\mathbf{U}}_2$ is the $m \times (m - n)$ matrix corresponding to the unwanted eigenvectors. Further, considering the partition of $\mathbf{\Lambda}$ as $\mathbf{\Lambda} = \begin{bmatrix} \mathbf{\Lambda}_1 & 0 \\ 0 & \mathbf{\Lambda}_2 \end{bmatrix}$ where $\mathbf{\Lambda}_1$ is the $n \times n$ diagonal matrix comprising of the wanted eigenvalues and $\mathbf{\Lambda}_2$ is the $(m - n) \times (m - n)$ diagonal matrix comprising of the unwanted eigenvalues. We have $\mathbf{H} = \hat{\mathbf{U}}_1 \mathbf{\Lambda}_1 \hat{\mathbf{U}}_1^\dagger + \hat{\mathbf{U}}_2 \mathbf{\Lambda}_2 \hat{\mathbf{U}}_2^\dagger$. Consequently we can write

$$\|\mathbf{R}^{(i)}\| = \|(\mathbf{I} - \mathbf{X}^{(i)}\mathbf{X}^{(i)\dagger})\mathbf{H}\mathbf{X}^{(i)}\| \quad (32)$$

$$= \|(\mathbf{I} - \mathbf{X}^{(i)}\mathbf{X}^{(i)\dagger})(\hat{\mathbf{U}}_1 \mathbf{\Lambda}_1 \hat{\mathbf{U}}_1^\dagger + \hat{\mathbf{U}}_2 \mathbf{\Lambda}_2 \hat{\mathbf{U}}_2^\dagger)\mathbf{X}^{(i)}\| \quad (33)$$

$$\leq \|(\mathbf{I} - \mathbf{X}^{(i)}\mathbf{X}^{(i)\dagger})\hat{\mathbf{U}}_1\| \|\mathbf{\Lambda}_1\| \|\hat{\mathbf{U}}_1^\dagger \mathbf{X}^{(i)}\| + \|(\mathbf{I} - \mathbf{X}^{(i)}\mathbf{X}^{(i)\dagger})\hat{\mathbf{U}}_2\| \|\mathbf{\Lambda}_2\| \|\hat{\mathbf{U}}_2^\dagger \mathbf{X}^{(i)}\| \quad (34)$$

Using the fact that $\sin \angle(\mathcal{S}^{(i)}, \mathcal{S}) = \|(\mathbf{I} - \mathbf{X}^{(i)}\mathbf{X}^{(i)\dagger})\hat{\mathbf{U}}_1\| = \|\hat{\mathbf{U}}_2^\dagger \mathbf{X}^{(i)}\|$ and the inequalities $\|\hat{\mathbf{U}}_1^\dagger \mathbf{X}^{(i)}\| \leq 1$, $\|(\mathbf{I} - \mathbf{X}^{(i)}\mathbf{X}^{(i)\dagger})\hat{\mathbf{U}}_2\| \leq 1$ we can write

$$\|\mathbf{R}^{(i)}\| \leq \sin \angle(\mathcal{S}^{(i)}, \mathcal{S}) (\|\mathbf{\Lambda}_1\| + \|\mathbf{\Lambda}_2\|) \leq 2\|\mathbf{H}\| \sin \angle(\mathcal{S}^{(i)}, \mathcal{S}) \quad (35)$$

\square

Theorem 3.3. *The necessary condition for $\angle(\underline{\mathcal{S}}^{(i+1)}, \mathcal{S}) < \angle(\mathcal{S}^{(i)}, \mathcal{S})$ for the case of residual-based Chebyshev filtering approach can be written as*

$$|C_p(\lambda_n)| - |C_p(\lambda_{n+1})| > 2\|\mathbf{H}\| \gamma_m \tilde{\eta}_p \left(1 + \tan \angle(\mathcal{S}^{(i)}, \mathcal{S})\right) \quad (36)$$

If this inequality is satisfied for $i = i_0$ then it holds for all $i > i_0$

Proof. As a consequence of Lemmas 3.2 to 3.4 we have $\|\hat{\Delta}_p^{(i)}\| \leq 2\|\mathbf{H}\| \gamma_m \tilde{\eta}_p \sin \angle(\mathcal{S}^{(i)}, \mathcal{S})$ and in order to have $\angle(\underline{\mathcal{S}}^{(i+1)}, \mathcal{S}) < \angle(\mathcal{S}^{(i)}, \mathcal{S})$ from Eq. (4) we require

$$|C_p(\lambda_n)| - |C_p(\lambda_{n+1})| > 2\|\mathbf{H}\| \gamma_m \tilde{\eta}_p \left(1 + \tan \angle(\mathcal{S}^{(i)}, \mathcal{S})\right) \quad (37)$$

We note that if this inequality is satisfied for some $i = i_0$ then it holds for all $i > i_0$ as the RHS decreases with decreasing $\angle(\mathcal{S}^{(i)}, \mathcal{S})$ and hence we conclude that the R-ChFSI method can converge under approximations where the ChFSI method fails. □

3.3. Generalized Eigenvalue Problems

We now analyze the case of a Hermitian generalized eigenproblem in Eq. (1) given by $\mathbf{A}\mathbf{u}_i = \lambda_i \mathbf{B}\mathbf{u}_i$ or equivalently $\mathbf{H}\mathbf{u}_i = \lambda_i \mathbf{u}_i$ with $\mathbf{H} = \mathbf{B}^{-1}\mathbf{A}$. In constructing a subspace rich in the desired eigenvectors using Chebyshev filtered subspace iteration approach, we consider the specific case of approximating \mathbf{B}^{-1} with a matrix \mathbf{D}^{-1} such that $\mathbf{D}^{-1}\mathbf{B} \approx \mathbf{I}$ in evaluating the matrix product $\mathbf{H}\mathbf{Y}_k^{(i)}$ within the Chebyshev recurrence relation defined by Eq. (3). We note that specific forms of the approximation, such as choosing \mathbf{D} to be diagonal or block diagonal, can give significant performance benefits.

3.3.1. Traditional Chebyshev filtering approach with inexact matrix-products involving \mathbf{D}^{-1}

Using the approximation \mathbf{D}^{-1} for \mathbf{B}^{-1} , the construction of filtered subspace using the recurrence relation in Eq. (3) is now accomplished by defining $\underline{\mathbf{Y}}_k^{(i)} = C_k(\mathbf{D}^{-1}\mathbf{A})\mathbf{X}^{(i)}$, where $k = 2, \dots, p$, and subsequently the 2-term recurrence relation can be written as

$$\underline{\mathbf{Y}}_{k+1}^{(i)} = a_k \mathbf{D}^{-1} \mathbf{A} \underline{\mathbf{Y}}_k^{(i)} + b_k \underline{\mathbf{Y}}_k^{(i)} + c_k \underline{\mathbf{Y}}_{k-1}^{(i)} \quad (38)$$

with the initial conditions $\underline{\mathbf{Y}}_0^{(i)} = \mathbf{X}^{(i)}$ and $\underline{\mathbf{Y}}_1^{(i)} = \sigma_1 \frac{\mathbf{D}^{-1}\mathbf{A} - c\mathbf{I}}{e} \mathbf{X}^{(i)}$. This allows us to write a recurrence relation for $\Delta_k^{(i)} = \underline{\mathbf{Y}}_k^{(i)} - \mathbf{Y}_k^{(i)}$ as

$$\Delta_{k+1}^{(i)} = a_k \mathbf{H} \Delta_k^{(i)} + b_k \Delta_k^{(i)} + c_k \Delta_{k-1}^{(i)} + a_k \left(\mathbf{D}^{-1} \mathbf{A} \underline{\mathbf{Y}}_k^{(i)} - \mathbf{B}^{-1} \mathbf{A} \underline{\mathbf{Y}}_k^{(i)} \right) \quad (39)$$

with the initial conditions $\Delta_0^{(i)} = \Delta_1^{(i)} = 0$.

Theorem 3.4. *The spectral norm of the error $\Delta_k^{(i)} = \underline{\mathbf{Y}}_k^{(i)} - \mathbf{Y}_k^{(i)}$ in the subspace construction using inexact matrix products of the recurrence relation Eq. (3) involving \mathbf{D}^{-1} satisfies $\|\Delta_k^{(i)}\| \leq \zeta \eta_k$ for $k = 0, 1, \dots, p$ where η_k is some finite constant that depends on k and $\zeta = \|\mathbf{D}^{-1} - \mathbf{B}^{-1}\|$*

Proof. We argue by induction that $\|\Delta_k^{(i)}\| \leq \zeta \eta_k$ where η_k is some finite constant that depends on k . To this end, assuming the induction hypothesis for $k = r-1$ and $k = r$, we have $\|\Delta_{r-1}^{(i)}\| \leq \zeta \eta_{r-1}$ and $\|\Delta_r^{(i)}\| \leq \zeta \eta_r$.

Subsequently, the following inequality is true for $\|\mathbf{\Delta}_{r+1}^{(i)}\|$ from Eq. (39)

$$\|\mathbf{\Delta}_{r+1}^{(i)}\| \leq |a_r| \|\mathbf{H}\| \eta_r \zeta + |b_r| \eta_r \zeta + |c_r| \eta_{r-1} \zeta + |a_r| \|\mathbf{D}^{-1} \mathbf{A} \mathbf{Y}_r^{(i)} - \mathbf{B}^{-1} \mathbf{A} \mathbf{Y}_r^{(i)}\| \quad (40)$$

$$\leq |a_r| \|\mathbf{H}\| \eta_r \zeta + |b_r| \eta_r \zeta + |c_r| \eta_{r-1} \zeta + |a_r| \|\mathbf{A}\| \|\mathbf{Y}_r^{(i)}\| \zeta \quad (41)$$

We further note that $\|\mathbf{Y}_r^{(i)}\| = \|\mathbf{\Delta}_r^{(i)} + \mathbf{Y}_r^{(i)}\| \leq \zeta \eta_r + \|\mathbf{Y}_r^{(i)}\| \leq \zeta \eta_r + \|C_r(\mathbf{H}) \mathbf{X}^{(i)}\| \leq \zeta \eta_r + \|C_r(\mathbf{H})\|$, and consequently we can write

$$\|\mathbf{\Delta}_{r+1}^{(i)}\| \leq [|a_r| \|\mathbf{H}\| \eta_r + |b_r| \eta_r + |c_r| \eta_{r-1} + |a_r| \|\mathbf{H}\| (\zeta \eta_r + \|C_r(\mathbf{H})\|)] \zeta \quad (42)$$

Defining $\eta_{r+1} = |a_r| \|\mathbf{H}\| \eta_r + |b_r| \eta_r + |c_r| \eta_{r-1} + |a_r| \|\mathbf{H}\| (\zeta \eta_r + \|C_r(\mathbf{H}) \mathbf{B}^{-\frac{1}{2}}\|)$ we have $\|\mathbf{\Delta}_{r+1}^{(i)}\| \leq \zeta \eta_{r+1}$ from the above equation. Hence using induction, we argue that $\|\mathbf{\Delta}_k^{(i)}\| \leq \zeta \eta_k$ for $k = 0, 1, \dots, p$ \square

We now discuss this result in the context of Eq. (6). Without loss of generality, we assume that our initial guess at $i = 0$ satisfies Eq. (6). While Eq. (6) is satisfied this allows for $\angle(\mathcal{S}^{(i)}, \mathcal{S})$ to decrease as i increases, but we note that the RHS of Eq. (6) does not monotonically decrease with $\angle(\mathcal{S}^{(i)}, \mathcal{S})$ and in fact increases as $\angle(\mathcal{S}^{(i)}, \mathcal{S})$ approaches 0. Thus, it stands to reason that beyond a certain value of $\angle(\mathcal{S}^{(i)}, \mathcal{S})$ Eq. (6) no longer holds, and we cannot approach the wanted eigenspace beyond this point. Assuming that $\zeta \eta_p \ll |C_p(\lambda_n)| - |C_p(\lambda_{n+1})|$ we estimate that the closest angle that can be achieved is

$$\angle(\mathcal{S}^{(i)}, \mathcal{S}) \approx \frac{\zeta \eta_p}{|C_p(\lambda_n)| - |C_p(\lambda_{n+1})|} \quad (43)$$

We now propose a residual-based reformulation of ChFSI for the generalized eigenvalue problem and argue that the proposed method does not suffer from this limitation.

3.3.2. Proposed residual-based Chebyshev filtering approach for generalized eigenproblem

We now propose a residual-based reformulation of the recurrence relation defined in Eq. (3). To this end we redefine the residual $\mathbf{R}_k^{(i)} = \mathbf{B}^{-1} \mathbf{D} (C_k(\mathbf{H}) \mathbf{X}^{(i)} - \mathbf{X}^{(i)} C_k(\mathbf{\Lambda}^{(i)})) = \mathbf{B}^{-1} \mathbf{D} (\mathbf{Y}_k^{(i)} - \mathbf{X}^{(i)} \mathbf{\Lambda}_k^{(i)})$ for $k = 0, \dots, p$, where we have defined $\mathbf{\Lambda}_k^{(i)} = C_k(\mathbf{\Lambda}^{(i)})$.

Proposition 3.2. *The recurrence relation given by Eq. (3) can be reformulated in terms of the $\mathbf{BR}_k^{(i)} = \mathbf{D} (\mathbf{Y}_k^{(i)} - \mathbf{X}^{(i)} \mathbf{\Lambda}_k^{(i)})$ as*

$$\mathbf{BR}_{k+1}^{(i)} = a_k \mathbf{D} \mathbf{H} \mathbf{D}^{-1} \mathbf{BR}_k^{(i)} + b_k \mathbf{BR}_k^{(i)} + c_k \mathbf{BR}_{k-1}^{(i)} + a_k \mathbf{D} \mathbf{B}^{-1} \mathbf{R}^{(i)} \mathbf{\Lambda}_k^{(i)} \quad (44)$$

where $\mathbf{BR}_0^{(i)} = 0$ and $\mathbf{BR}_1^{(i)} = \frac{\sigma_1}{e} \mathbf{D} \mathbf{B}^{-1} \mathbf{R}^{(i)}$ with $\mathbf{R}^{(i)} = \mathbf{A} \mathbf{X}^{(i)} - \mathbf{B} \mathbf{X}^{(i)} \mathbf{\Lambda}^{(i)}$.

Proof. The recurrence relation for $\mathbf{\Lambda}_k^{(i)} = C_k(\mathbf{\Lambda}^{(i)})$ can be written as

$$\mathbf{\Lambda}_{k+1}^{(i)} = a_k \mathbf{\Lambda}_k^{(i)} \mathbf{\Lambda}^{(i)} + b_k \mathbf{\Lambda}_k^{(i)} + c_k \mathbf{\Lambda}_{k-1}^{(i)}$$

Multiplying with $\mathbf{X}^{(i)}$ and subtracting from Eq. (3), we have

$$\begin{aligned}\mathbf{Y}_{k+1}^{(i)} - \mathbf{X}^{(i)} \boldsymbol{\Lambda}_{k+1}^{(i)} &= a_k (\mathbf{H} \mathbf{Y}_k^{(i)} - \mathbf{X}^{(i)} \boldsymbol{\Lambda}_k^{(i)} \boldsymbol{\Lambda}^{(i)}) + b_k (\mathbf{Y}_k^{(i)} - \mathbf{X}^{(i)} \boldsymbol{\Lambda}_k^{(i)}) + c_k (\mathbf{Y}_{k-1}^{(i)} - \mathbf{X}^{(i)} \boldsymbol{\Lambda}_k^{(i)}) \\ \implies \mathbf{D}^{-1} \mathbf{B} \mathbf{R}_{k+1}^{(i)} &= a_k \mathbf{H} \mathbf{D}^{-1} \mathbf{B} \mathbf{R}_k^{(i)} + b_k \mathbf{D}^{-1} \mathbf{B} \mathbf{R}_k^{(i)} + c_k \mathbf{D}^{-1} \mathbf{B} \mathbf{R}_{k-1}^{(i)} + a_k \mathbf{B}^{-1} \mathbf{R}^{(i)} \boldsymbol{\Lambda}_k^{(i)} \\ \implies \mathbf{B} \mathbf{R}_{k+1}^{(i)} &= a_k \mathbf{D} \mathbf{H} \mathbf{D}^{-1} \mathbf{B} \mathbf{R}_k^{(i)} + b_k \mathbf{B} \mathbf{R}_k^{(i)} + c_k \mathbf{B} \mathbf{R}_{k-1}^{(i)} + a_k \mathbf{D} \mathbf{B}^{-1} \mathbf{R}^{(i)} \boldsymbol{\Lambda}_k^{(i)}\end{aligned}$$

□

After computing $\mathbf{B} \mathbf{R}_p^{(i)}$ using this recurrence relation we can now evaluate $\mathbf{Y}_p^{(i)}$ using the relation $\mathbf{Y}_p^{(i)} = \mathbf{D}^{-1} \mathbf{B} \mathbf{R}_p^{(i)} + \mathbf{X}^{(i)} \boldsymbol{\Lambda}_p^{(i)}$. We note that using approximation $\mathbf{D} \mathbf{B}^{-1} \approx \mathbf{I}$ we can write the following recurrence relation

$$\mathbf{B} \mathbf{R}_{k+1}^{(i)} = a_k \mathbf{A} \mathbf{D}^{-1} \mathbf{B} \mathbf{R}_k^{(i)} + b_k \mathbf{B} \mathbf{R}_k^{(i)} + c_k \mathbf{B} \mathbf{R}_{k-1}^{(i)} + a_k \mathbf{R}^{(i)} \boldsymbol{\Lambda}_k^{(i)} \quad (45)$$

with $\mathbf{B} \mathbf{R}_0^{(i)} = 0$ and $\mathbf{B} \mathbf{R}_1^{(i)} = \frac{2\sigma_2}{e} \mathbf{R}^{(i)}$ and consequently, we have $\mathbf{Y}_k^{(i)} = \mathbf{D}^{-1} \mathbf{B} \mathbf{R}_k^{(i)} + \mathbf{X}^{(i)} \boldsymbol{\Lambda}_k^{(i)}$. Note that this recurrence relation does not require the evaluation \mathbf{B}^{-1} . We can now write a recurrence relation for $\boldsymbol{\Delta}_k^{(i)} = \mathbf{Y}_k^{(i)} - \mathbf{Y}_k = \mathbf{D}^{-1} \mathbf{B} (\mathbf{R}_k^{(i)} - \mathbf{R}_k^{(i)})$ as

$$\boldsymbol{\Delta}_{k+1}^{(i)} = a_k \mathbf{H} \boldsymbol{\Delta}_k^{(i)} + b_k \boldsymbol{\Delta}_k^{(i)} + c_k \boldsymbol{\Delta}_{k-1}^{(i)} + a_k (\mathbf{I} - \mathbf{D} \mathbf{B}^{-1}) (\mathbf{R}^{(i)} \boldsymbol{\Lambda}_k^{(i)} + \mathbf{A} \mathbf{D}^{-1} \mathbf{B} \mathbf{R}_k^{(i)}) \quad (46)$$

where $\boldsymbol{\Delta}_0^{(i)} = 0$ and $\boldsymbol{\Delta}_1^{(i)} = \frac{2\sigma_2}{e} (\mathbf{I} - \mathbf{D} \mathbf{B}^{-1}) \mathbf{R}^{(i)}$.

Lemma 3.5. *The spectral norm of the error $\boldsymbol{\Delta}_k^{(i)} = \mathbf{Y}_k^{(i)} - \mathbf{Y}_k^{(i)}$ in the subspace construction using recurrence relation given by Eq. (45) satisfies $\|\boldsymbol{\Delta}_k^{(i)}\| \leq \tilde{\zeta} \tilde{\eta}_k \|\mathbf{R}^{(i)}\|$ for $k = 0, 1, \dots, p$ where $\tilde{\eta}_k$ is some finite constant that depends on k and $\tilde{\zeta} = \|\mathbf{I} - \mathbf{D} \mathbf{B}^{-1}\|$.*

Proof. We argue by induction that $\|\boldsymbol{\Delta}_k^{(i)}\| \leq \tilde{\zeta} \tilde{\eta}_k \|\mathbf{R}^{(i)}\|$ where $\tilde{\eta}_k$ is some non-zero finite constant that depends on k . To this end, assuming the induction hypothesis for $k = r - 1$ and $k = r$, we have $\|\boldsymbol{\Delta}_r^{(i)}\| \leq \tilde{\zeta} \tilde{\eta}_r \|\mathbf{R}^{(i)}\|$ and $\|\boldsymbol{\Delta}_{r-1}^{(i)}\| \leq \tilde{\zeta} \tilde{\eta}_{r-1} \|\mathbf{R}^{(i)}\|$. Subsequently, the following inequality is true for $\|\boldsymbol{\Delta}_{r+1}^{(i)}\|$ from Eq. (46)

$$\begin{aligned}\|\boldsymbol{\Delta}_{r+1}^{(i)}\| &\leq |a_r| \|\mathbf{H}\| \tilde{\eta}_r \tilde{\zeta} \|\mathbf{R}^{(i)}\| + |b_r| \tilde{\eta}_r \tilde{\zeta} \|\mathbf{R}^{(i)}\| + |c_r| \tilde{\eta}_{r-1} \tilde{\zeta} \|\mathbf{R}^{(i)}\| + |a_r| \|(\mathbf{I} - \mathbf{D} \mathbf{B}^{-1}) (\mathbf{R}^{(i)} \boldsymbol{\Lambda}_r^{(i)} + \mathbf{A} \mathbf{D}^{-1} \mathbf{B} \mathbf{R}_r^{(i)})\| \\ &\leq |a_r| \|\mathbf{H}\| \tilde{\eta}_r \tilde{\zeta} \|\mathbf{R}^{(i)}\| + |b_r| \tilde{\eta}_r \tilde{\zeta} \|\mathbf{R}^{(i)}\| + |c_r| \tilde{\eta}_{r-1} \tilde{\zeta} \|\mathbf{R}^{(i)}\| + |a_r| \tilde{\zeta} \|\mathbf{R}^{(i)} \boldsymbol{\Lambda}_r^{(i)} + \mathbf{A} \mathbf{D}^{-1} \mathbf{B} \mathbf{R}_r^{(i)}\| \\ &\leq |a_r| \|\mathbf{H}\| \tilde{\eta}_r \tilde{\zeta} \|\mathbf{R}^{(i)}\| + |b_r| \tilde{\eta}_r \tilde{\zeta} \|\mathbf{R}^{(i)}\| + |c_r| \tilde{\eta}_{r-1} \tilde{\zeta} \|\mathbf{R}^{(i)}\| + |a_r| \tilde{\zeta} \left(\|\boldsymbol{\Lambda}_r^{(i)}\| \|\mathbf{R}^{(i)}\| + \|\mathbf{A} \mathbf{D}^{-1} \mathbf{B}\| \|\mathbf{R}_r^{(i)}\| \right)\end{aligned}$$

We further note that using Lemma 3.2 we can write $\|\mathbf{R}_r^{(i)}\| = \|\boldsymbol{\Delta}_r^{(i)} + \mathbf{R}_r^{(i)}\| \leq \tilde{\zeta} \tilde{\eta}_r \|\mathbf{R}^{(i)}\| + \|\mathbf{R}_r^{(i)}\| \leq \tilde{\zeta} \tilde{\eta}_r \|\mathbf{R}^{(i)}\| + f_r \|\mathbf{R}^{(i)}\|$, and consequently we can write

$$\|\boldsymbol{\Delta}_{r+1}^{(i)}\| \leq \left[|a_r| \|\mathbf{H}\| \tilde{\eta}_r + |b_r| \tilde{\eta}_r + |c_r| \tilde{\eta}_{r-1} + |a_r| (\|\boldsymbol{\Lambda}_r^{(i)}\| + \|\mathbf{A} \mathbf{D}^{-1} \mathbf{B}\| (\tilde{\zeta} \tilde{\eta}_r + f_r)) \right] \tilde{\zeta} \|\mathbf{R}^{(i)}\| \quad (47)$$

Defining $\tilde{\eta}_{r+1} = |a_r| \|\mathbf{H}\| \tilde{\eta}_r + |b_r| \tilde{\eta}_r + |c_r| \tilde{\eta}_{r-1} + |a_r| (\|\boldsymbol{\Lambda}_r^{(i)}\| + \|\mathbf{A} \mathbf{D}^{-1} \mathbf{B}\| (\tilde{\zeta} \tilde{\eta}_r + f_r))$. Hence, using induction, we argue that $\|\boldsymbol{\Delta}_{k+1}^{(i)}\| \leq \tilde{\zeta} \tilde{\eta}_{k+1} \|\mathbf{R}^{(i)}\|$ for $k = 0, 1, \dots, p$. □

Theorem 3.5. *The necessary condition for $\angle(\underline{\mathcal{S}}^{(i+1)}, \mathcal{S}) < \angle(\mathcal{S}^{(i)}, \mathcal{S})$ for the case of residual-based Chebyshev filtering approach can be written as*

$$|C_p(\lambda_n)| - |C_p(\lambda_{n+1})| > 2\|\mathbf{H}\| \tilde{\zeta} \tilde{\eta}_p \left(1 + \tan \angle(\mathcal{S}^{(i)}, \mathcal{S})\right) \quad (48)$$

If this inequality is satisfied for at $i = i_0$ then it holds for all $i > i_0$

Proof. As a consequence of Lemmas 3.2, 3.4 and 3.5 we have $\|\hat{\Delta}_p^{(i)}\| \leq 2\|\mathbf{H}\| \tilde{\zeta} \tilde{\eta}_p \sin \angle(\mathcal{S}^{(i)}, \mathcal{S})$ and in order to have $\angle(\underline{\mathcal{S}}^{(i+1)}, \mathcal{S}) < \angle(\mathcal{S}^{(i)}, \mathcal{S})$ from Eq. (4) we require

$$|C_p(\lambda_n)| - |C_p(\lambda_{n+1})| > 2\|\mathbf{H}\| \tilde{\zeta} \tilde{\eta}_p \left(1 + \tan \angle(\mathcal{S}^{(i)}, \mathcal{S})\right) \quad (49)$$

We note that if this inequality is satisfied for some $i = i_0$ then it holds for all $i > i_0$ as the RHS decreases with decreasing $\angle(\mathcal{S}^{(i)}, \mathcal{S})$ and hence we conclude that the R-ChFSI method can converge under approximations where the ChFSI method fails even for generalized eigenvalue problems. □

4. Results and Discussion

We present a detailed evaluation of the accuracy and efficiency achieved by the proposed residual-based Chebyshev filtered subspace iteration (R-ChFSI) method for solving real symmetric and complex Hermitian eigenvalue problems both for standard and generalized eigenproblems. We compare the performance of the R-ChFSI method with that of traditional ChFSI approaches, demonstrating its improved accuracy even when employing inexact matrix-vector products. Additionally, we investigate its performance on ‘‘Eos’’ NVIDIA DGX SuperPOD with NVIDIA H100 GPUs and Intel Xeon Platinum 8480C CPUs, demonstrating its ability to maintain high accuracy while achieving greater computational efficiency. For generalized eigenvalue problems of the form $\mathbf{Ax} = \lambda\mathbf{Bx}$, we explore the use of diagonal approximations of \mathbf{B} to compute its inverse for the subspace construction step within both the ChFSI and R-ChFSI methods, showing that the latter can achieve significantly lower residual tolerances. For all our benchmark studies reported in this work, we consider the sparse matrix eigenvalue problems that arise from higher-order finite-element discretization of Kohn-Sham density functional theory (DFT) [32, 38, 55, 70–74].

In the following subsections, we focus on specific problem classes, starting with the results for standard eigenvalue problems, including the cases of real symmetric and complex Hermitian matrices, followed by generalized eigenvalue problems, where we assess the convergence behavior and the performance of the ChFSI and the R-ChFSI methods. To this end, we consider a set of three benchmark systems whose dimensions are summarized in Table 1. These eigenvalue problems are obtained from the finite-element discretization of the Kohn-Sham DFT equations for the periodic supercells of various sizes for body-centered cubic (BCC) Molybdenum systems with a single vacancy. For all the benchmarks we utilize a Chebyshev polynomial degree of 75.

System	# of DoFs (m)	# of wanted eigenvectors (n)	Subspace dimension
(1)	1728000	3000	3600
(2)	4251528	7000	8400
(3)	7645373	14000	16800

Table 1: Dimensions of the benchmark problems considered. These correspond to 3 material systems comprising $6 \times 6 \times 6$, $8 \times 8 \times 8$ and $10 \times 10 \times 10$ body-centered-cubic (BCC) periodic supercells of Molybdenum with a single vacancy

4.1. Standard Eigenvalue Problems

We now evaluate the accuracy and performance of the proposed R-ChFSI method as described in Algorithm 2 for solving the standard eigenvalue problems. We choose the eigenproblem encountered in using the higher-order finite-element discretization of Kohn-Sham DFT as outlined in Das et al. [38], Motamarri et al. [55]. We begin by comparing the R-ChFSI method to the ChFSI method using FP32 and TF32 arithmetic. We demonstrate below that the R-ChFSI method with FP32 and TF32 arithmetic converges to the desired residual tolerance in a similar number of iterations as that of the ChFSI method employing FP64 arithmetic. In contrast, the ChFSI method with FP32 and TF32 arithmetic fails to reach the same residual tolerance as that of the ChFSI method with FP64 arithmetic.

4.1.1. Symmetric Eigenvalue Problems

We now consider the finite-element discretization of the Kohn-Sham DFT equations sampled at the origin (Gamma point) of the Brillouin zone for the material systems described in Table 1. This ensures that the resulting discretized equation is a real symmetric eigenvalue problem. The computation of the matrix multi-vector products with FP64 arithmetic is performed according to the methodology prescribed by [38, 55]. When using FP32 arithmetic to evaluate $\mathbf{A}\mathbf{R}_Y$ in Line 13 of Algorithm 2, the data structures storing the matrix \mathbf{A} and multi-vectors \mathbf{R}_X and \mathbf{R}_Y are in FP32 format and the BLAS calls used to perform $\mathbf{A}\mathbf{R}_Y$ are replaced with corresponding FP32 variants while the addition and scaling of multi-vectors is done using FP64 arithmetic. For TF32 arithmetic on NVIDIA GPUs we replace the `cublasSgemm` and its strided/batched variants with `cublasGemmEx` and its strided/batched variants with `computeType` set to `CUBLAS_COMPUTE_32F_FAST_TF32`. From Fig. 1, we observe that for all the benchmark systems summarized in Table 1, the accuracy achieved by the FP32 and TF32 variants for the R-ChFSI method is comparable to that achieved by the FP64 variant of the ChFSI method, whereas the FP32 and TF32 variants of the ChFSI method show significant reduction in achievable residual tolerance. We also note that the rate of convergence that is achieved by the FP32 and TF32 variants for the R-ChFSI method is comparable to that achieved by the FP64 variant of the ChFSI method. We also report the speedups achieved by the FP32 and

Algorithm 2: Reformulated ChFSI (R-ChFSI) Procedure for standard Hermitian eigenvalue problems

Input:

Chebyshev polynomial order p , estimates of the bounds of the eigenspectrum $\lambda_{max}, \lambda_{min}$, estimate of the upper bound of the wanted spectrum λ_T and the initial guess of eigenvectors $\mathbf{X}^{(i)}$ and eigenvalues $\Lambda^{(i)}$

Result: The filtered subspace $\mathbf{Y}_p^{(i)}$

Temporary Variable: $\mathbf{X}, \mathbf{Y}, \mathbf{R}_X, \mathbf{R}_Y, \Lambda_X$ and Λ_Y

```

1  $e \leftarrow \frac{\lambda_{max} - \lambda_T}{2}; c \leftarrow \frac{\lambda_{max} + \lambda_T}{2};$ 
2  $\sigma \leftarrow \frac{e}{\lambda_{min} - c};$ 
3  $\sigma_1 \leftarrow \sigma;$ 
4  $\gamma \leftarrow \frac{2}{\sigma_1};$ 
5  $\mathbf{X} \leftarrow \mathbf{X}^{(i)};$ 
6  $\mathbf{Y} \leftarrow \mathbf{A}\mathbf{X}^{(i)} - \mathbf{X}^{(i)}\Lambda^{(i)};$ 
7  $\mathbf{R}_X \leftarrow \mathbf{0};$ 
8  $\mathbf{R}_Y \leftarrow \frac{2\sigma_1}{e}\mathbf{Y};$ 
9  $\Lambda_X \leftarrow \mathbf{I};$ 
10  $\Lambda_Y \leftarrow \frac{2\sigma_1}{e}(\Lambda^{(i)} - c\mathbf{I});$ 
11 for  $k \leftarrow 2$  to  $p$  do
12    $\sigma_2 \leftarrow \frac{1}{\gamma - \sigma};$ 
13    $\mathbf{R}_X \leftarrow \frac{2\sigma_2}{e}\mathbf{A}\mathbf{R}_Y - \frac{2\sigma_2}{e}c\mathbf{R}_Y - \sigma\sigma_2\mathbf{R}_X + \frac{2\sigma_2}{e}\mathbf{Y}\Lambda_Y;$ 
14    $\Lambda_X \leftarrow \frac{2\sigma_2}{e}\Lambda_Y\Lambda^{(i)} - \frac{2\sigma_2}{e}c\Lambda_Y - \sigma\sigma_2\Lambda_X;$ 
15   swap( $\mathbf{X}, \mathbf{Y}$ );
16   swap( $\Lambda_X, \Lambda_Y$ );
17    $\sigma = \sigma_2;$ 
18  $\mathbf{X} \leftarrow \mathbf{R}_Y + \mathbf{X}\Lambda_Y;$ 
19 return  $\mathbf{X}$ 

```

TF32 variants of ChFSI and R-ChFSI over the FP64 variant of ChFSI in Fig. 2 on NVIDIA H100 GPU accelerators. We note that we obtain similar speedups for both the ChFSI and R-ChFSI methods allowing us to conclude that the additional overheads in the R-ChFSI method are negligible. We have achieved speedups of up to 1.75x for the TF32 variant of the R-ChFSI method over the baseline implementation of the ChFSI method with FP64 arithmetic. We also report the speedups achieved by the FP32 variant of ChFSI and R-ChFSI over the FP64 variant of ChFSI in Fig. 3 on Intel Xeon Platinum 8480C CPUs. We note that the speedups of the R-ChFSI method are slightly lower than ChFSI method due to the additional overheads in the R-ChFSI method. We achieve speedups of up to 2.1x for the FP32 variant of the R-ChFSI method over the baseline implementation of the ChFSI method with FP64 arithmetic.

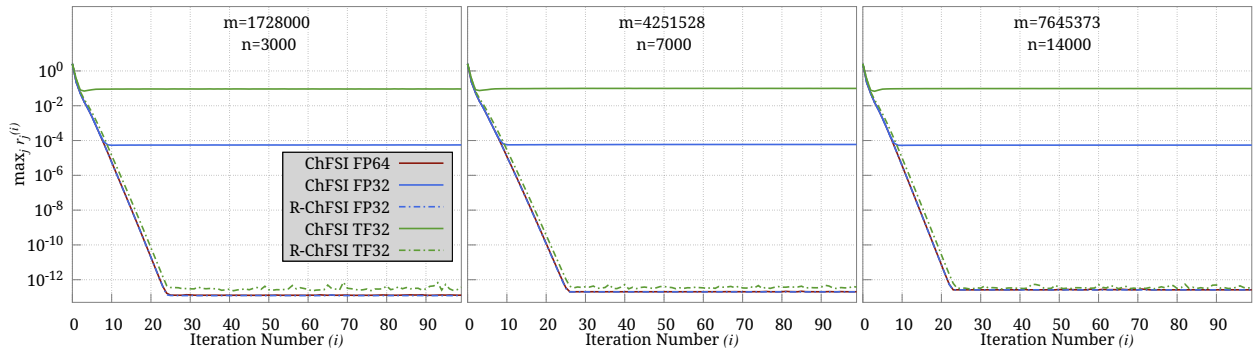


Figure 1: Plot of $\max_j r_j^{(i)} = \max_j \|\mathbf{A}\mathbf{x}_j^{(i)} - \epsilon_j^{(i)}\mathbf{x}_j^{(i)}\|$ as the iterations progress to solve the symmetric standard eigenvalue problem with various precisions for the benchmark systems described in Table 1.

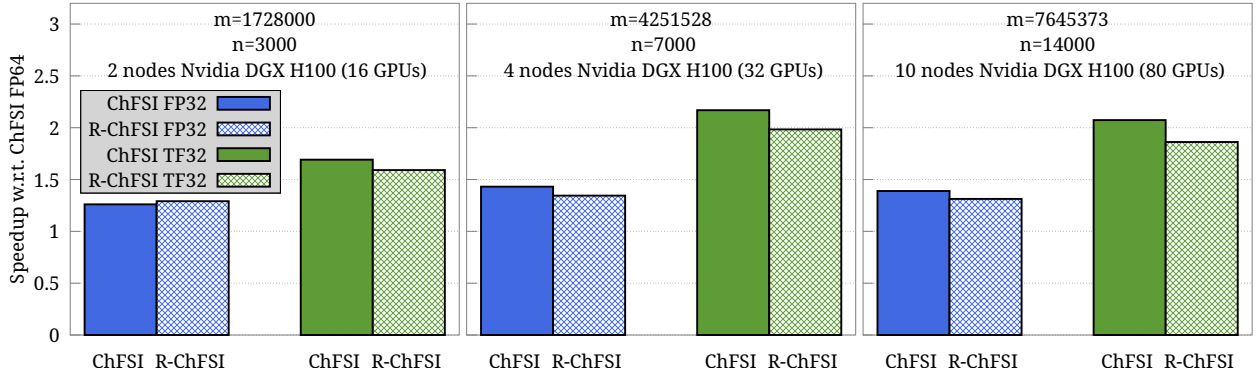


Figure 2: Speedups of lower precision ChFSI and R-ChFSI methods over the FP64 ChFSI method for subspace construction to solve the symmetric standard eigenvalue problem on GPUs for the benchmark systems described in Table 1.

4.1.2. Hermitian Eigenvalue Problems

We now consider the finite-element discretization of the Kohn-Sham DFT equations at a non-zero k -point [38] in the Brillouin zone for the systems described in Table 1. The resulting discretized equation is now a

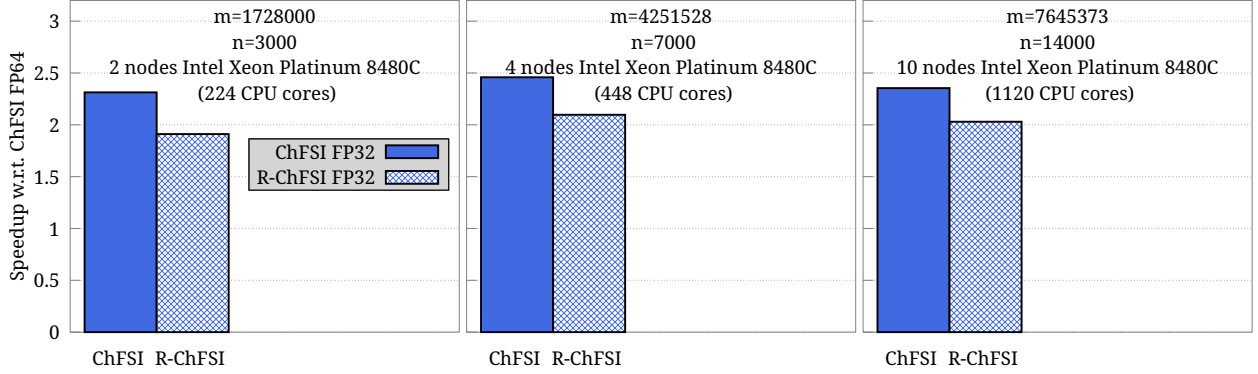


Figure 3: Speedups of lower precision ChFSI and R-ChFSI methods over the FP64 ChFSI method for subspace construction to solve the symmetric standard eigenvalue problem on CPUs for the benchmark systems described in Table 1.

complex Hermitian eigenvalue problem. The computation of the matrix multi-vector products with FP64 arithmetic is done according to the methodology prescribed by [38, 55]. When using FP32 arithmetic to evaluate $\mathbf{A}\mathbf{R}_\mathbf{Y}$ in Line 13 of Algorithm 2, the data structures storing the matrix \mathbf{A} and multi-vectors $\mathbf{R}_\mathbf{X}$ and $\mathbf{R}_\mathbf{Y}$ are in FP32 format and the BLAS calls used to perform $\mathbf{A}\mathbf{R}_\mathbf{Y}$ are replaced with corresponding FP32 variants while the addition and scaling of multi-vectors is done using FP64 arithmetic. For TF32 arithmetic on NVIDIA GPUs we replace the `cublasCgemm` and its strided/batched variants with `cublasGemmEx` and its strided/batched variants with `computeType` set to `CUBLAS_COMPUTE_32F_FAST_TF32`. From Fig. 4, we

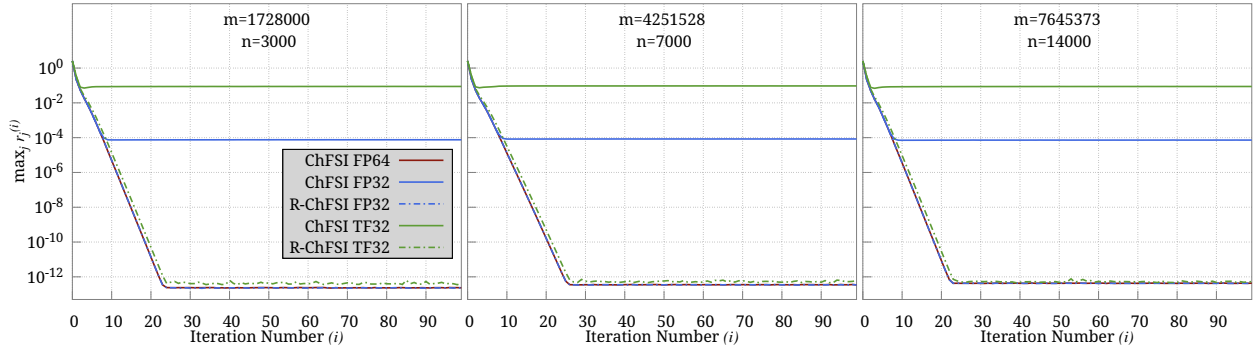


Figure 4: Plot of $\max_j r_j^{(i)} = \max_j \|\mathbf{A}\mathbf{x}_j^{(i)} - \epsilon_j^{(i)} \mathbf{x}_j^{(i)}\|$ as the iterations progress to solve the Hermitian standard eigenvalue problem for various precisions to solve the Hermitian standard eigenvalue problem for the benchmark systems described in Table 1.

observe that for all the benchmark systems summarized in Table 1, the accuracy achieved by the FP32 and TF32 variants for the R-ChFSI method is comparable to that achieved by the FP64 variant of the ChFSI method, whereas the FP32 and TF32 variants of the R-ChFSI method show a significant reduction in achievable residual tolerance. We also note that the rate of convergence that is achieved by the FP32 and TF32 variants for the R-ChFSI method is comparable to that achieved by the FP64 variant of the ChFSI.

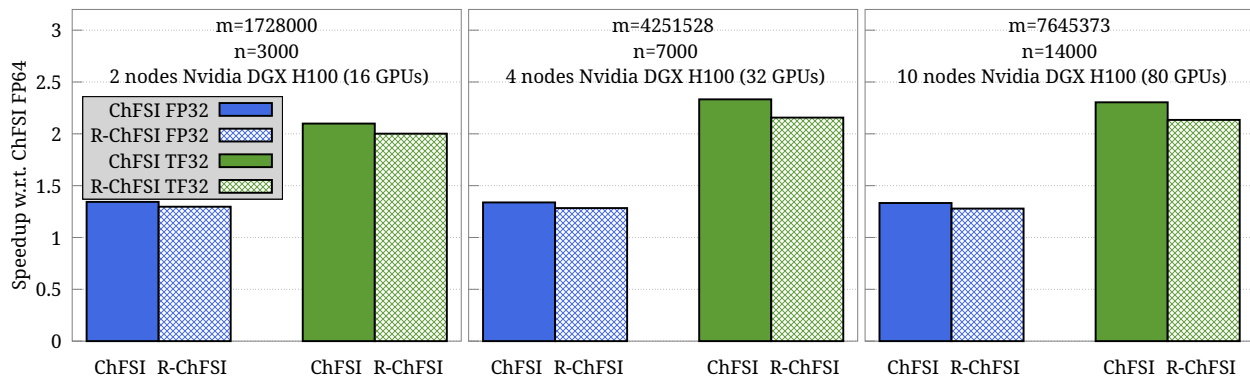


Figure 5: Speedups of lower precision ChFSI and R-ChFSI methods over the FP64 ChFSI method for subspace construction to solve the Hermitian standard eigenvalue problem on GPUs for the benchmark systems described in Table 1.

We also report the speedups achieved by the FP32 and TF32 variants of ChFSI and R-ChFSI over the FP64 variant of ChFSI in Fig. 5 on NVIDIA H100 GPU accelerators. We note that we obtain similar speedups for both the ChFSI and R-ChFSI methods allowing us to conclude that the additional overheads in the R-ChFSI method are negligible. We achieve speedups of up to 2.0x for the TF32 variant of the R-ChFSI method over the baseline implementation of the ChFSI method with FP64 arithmetic.

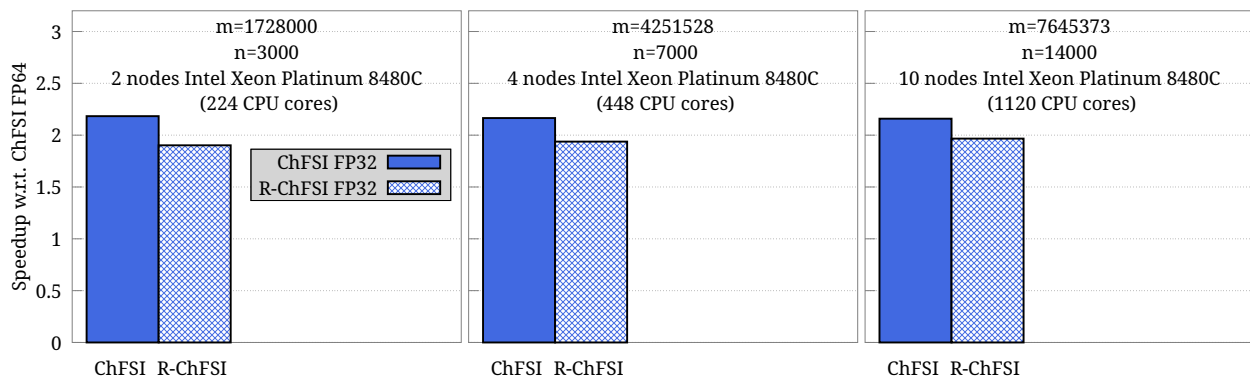


Figure 6: Speedups of lower precision ChFSI and R-ChFSI methods over the FP64 ChFSI method for subspace construction to solve the Hermitian standard eigenvalue problem on CPUs for the benchmark systems described in Table 1.

We also report the speedups achieved by the FP32 variant of ChFSI and R-ChFSI over the FP64 variant of ChFSI in Fig. 6 on Intel Xeon Platinum 8480C CPUs. We note that the speedups of the R-ChFSI method are slightly lower due to the additional overheads in the R-ChFSI method. We have achieved speedups of up to 2.0x for the FP32 variant of the R-ChFSI method over the baseline implementation of the ChFSI method with FP64 arithmetic.

4.2. Generalized Eigenvalue Problems

We now evaluate the accuracy and performance of the proposed R-ChFSI method for generalized eigenvalue problems as described in Algorithm 3 resulting from the higher-order finite-element discretized Kohn-Sham DFT equations. The generalized eigen problem arises in the finite-element discretization of DFT equations because of the non-orthogonality of the FE basis functions. We begin by comparing the R-ChFSI method to the ChFSI method using a diagonal approximation of the finite-element overlap matrix. To this end, we consider the set of three benchmark systems whose dimensions are summarized in Table 1. We demonstrate that the R-ChFSI method converges to a significantly lower residual tolerance than the ChFSI method when the diagonal approximation is employed for approximating the inverse overlap matrix during the subspace construction.

4.2.1. Symmetric Eigenvalue Problems

We now consider the finite-element discretization of the Kohn-Sham DFT equations at the origin (Gamma point) in the Brillouin zone for the systems described in Table 1. This ensures that the resulting discretized equation is a real symmetric eigenvalue problem. All the computations are done with FP64 according to the methodology prescribed by [38, 55].

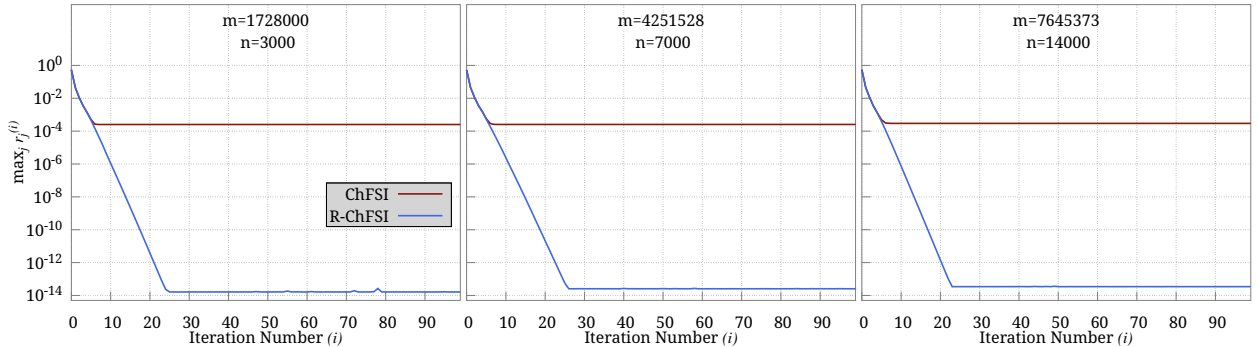


Figure 7: Plot of $\max_j r_j^{(i)} = \max_j \|\mathbf{A}\mathbf{x}_j^{(i)} - \epsilon_j^{(i)} \mathbf{B}\mathbf{x}_j^{(i)}\|$ as the iterations progress for the ChFSI method and the R-ChFSI method to solve the symmetric generalized eigenvalue problem for the benchmark systems described in Table 1.

From Fig. 7, we observe that for all the benchmark systems summarized in Table 1, the residual tolerance than can be achieved by the R-ChFSI method is nearly 10 orders of magnitude lower than what can be achieved using the ChFSI method when employing the diagonal approximation for the inverse overlap matrix. We also note that our proposed R-ChFSI algorithm allows us to construct the filtered subspace using lower precision and we report the residuals achieved by the FP32 and TF32 variants of R-ChFSI in Fig. 8. We also report the speedups achieved by the FP32 and TF32 variants of R-ChFSI over the FP64 variant of R-ChFSI in Fig. 9 on NVIDIA H100 GPU accelerators. We achieve speedups of up to 2.3x for the TF32 variant of the R-ChFSI method over the baseline implementation of the ChFSI method with FP64 arithmetic.

Algorithm 3: Reformulated ChFSI (R-ChFSI) Procedure for generalized eigenvalue problems**Input:**

Chebyshev polynomial order p , estimates of the bounds of the eigenspectrum $\lambda_{max}, \lambda_{min}$, estimate of the upper bound of the wanted spectrum λ_T and the initial guess of eigenvectors $\mathbf{X}^{(i)}$ and eigenvalues $\Lambda^{(i)}$

Result: The filtered subspace $\mathbf{Y}_p^{(i)}$

Temporary Variable: $\mathbf{X}, \mathbf{Y}, \mathbf{R}_X, \mathbf{R}_Y, \Lambda_X$ and Λ_Y

```
1  $e \leftarrow \frac{\lambda_{max} - \lambda_T}{2}; c \leftarrow \frac{\lambda_{max} + \lambda_T}{2};$ 
2  $\sigma \leftarrow \frac{e}{\lambda_{min} - c};$ 
3  $\sigma_1 \leftarrow \sigma;$ 
4  $\gamma \leftarrow \frac{2}{\sigma_1};$ 
5  $\mathbf{X} \leftarrow \mathbf{X}^{(i)};$ 
6  $\mathbf{Y} \leftarrow \mathbf{A}\mathbf{X}^{(i)} - \mathbf{B}\mathbf{X}^{(i)}\Lambda^{(i)};$ 
7  $\mathbf{R}_X \leftarrow 0;$ 
8  $\mathbf{R}_Y \leftarrow \frac{2\sigma_1}{e}\mathbf{Y};$ 
9  $\Lambda_X \leftarrow \mathbf{I};$ 
10  $\Lambda_Y \leftarrow \frac{2\sigma_1}{e}(\Lambda^{(i)} - c\mathbf{I});$ 
11 for  $k \leftarrow 2$  to  $p$  do
12    $\sigma_2 \leftarrow \frac{1}{\gamma - \sigma};$ 
13    $\mathbf{R}_X \leftarrow \frac{2\sigma_2}{e}\mathbf{A}\mathbf{D}^{-1}\mathbf{R}_Y - \frac{2\sigma_2}{e}c\mathbf{R}_Y - \sigma\sigma_2\mathbf{R}_X + \frac{2\sigma_2}{e}\mathbf{Y}\Lambda_Y;$ 
14    $\Lambda_X \leftarrow \frac{2\sigma_2}{e}\Lambda_Y\Lambda^{(i)} - \frac{2\sigma_2}{e}c\Lambda_Y - \sigma\sigma_2\Lambda_X;$ 
15   swap( $\mathbf{X}, \mathbf{Y}$ );
16   swap( $\Lambda_X, \Lambda_Y$ );
17    $\sigma = \sigma_2;$ 
18  $\mathbf{X} \leftarrow \mathbf{D}^{-1}\mathbf{R}_Y + \mathbf{X}\Lambda_Y;$ 
19 return  $\mathbf{X}$ 
```

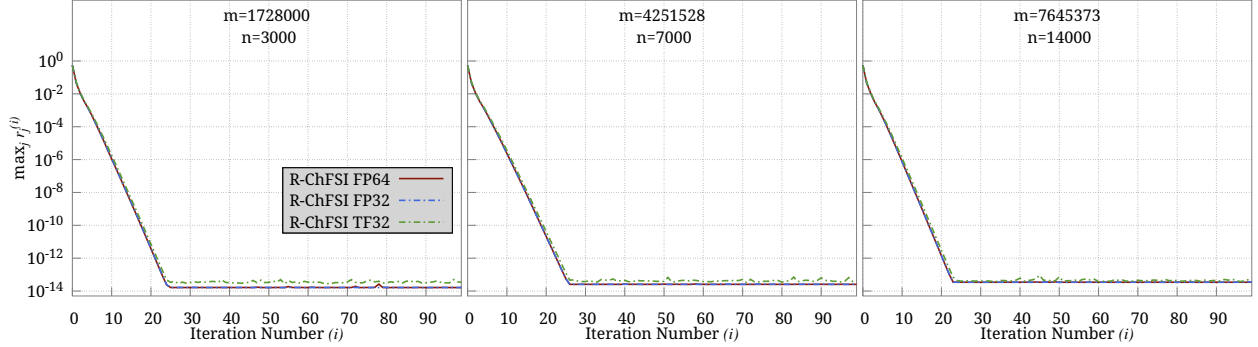


Figure 8: Plot of $\max_j r_j^{(i)} = \max_j \|\mathbf{A}\mathbf{x}_j^{(i)} - \epsilon_j^{(i)} \mathbf{B}\mathbf{x}_j^{(i)}\|$ as the iterations progress for the R-ChFSI method to solve the symmetric generalized eigenvalue problem with various precisions for the benchmark systems described in Table 1.

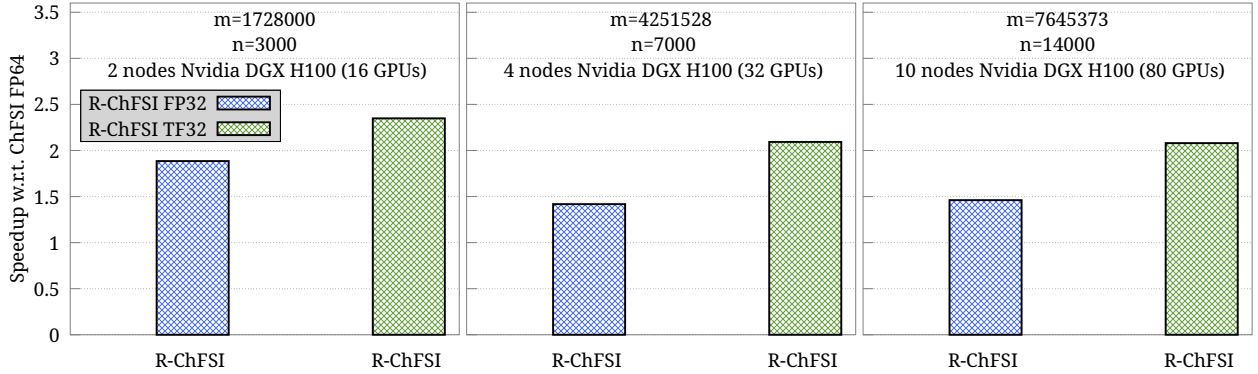


Figure 9: Speedups of lower precision R-ChFSI methods over the FP64 R-ChFSI method for subspace construction to solve the symmetric generalized eigenvalue problem for the benchmark systems described in Table 1.

4.2.2. Hermitian Eigenvalue Problems

We now consider the finite-element discretization of the Kohn-Sham DFT equations at a non-zero k -point [38] in the Brillouin zone for the systems described in Table 1. The resulting discretized equation is now a complex Hermitian eigenvalue problem. All the computations are done with FP64 according to the methodology prescribed by [38, 55]. From Fig. 10, we observe that for all the benchmark systems summarized in Table 1, even for Hermitian eigenvalue problems the residual tolerance than can be achieved by the R-ChFSI method is nearly 10 orders of magnitude lower than what can be achieved using the ChFSI method when employing the diagonal approximation for the inverse overlap matrix. We also note that our proposed R-ChFSI algorithm allows for us to construct the filtered subspace using lower precision and we report the residuals achieved by the FP32 and TF32 variants of R-ChFSI in Fig. 11. We also report the speedups achieved by the FP32 and TF32 variants of R-ChFSI over the FP64 variant of R-ChFSI in Fig. 12 on NVIDIA H100 GPU accelerators. We achieve speedups of up to 2.7x for the TF32 variant of the R-ChFSI method over the baseline implementation of the R-ChFSI method with FP64 arithmetic.

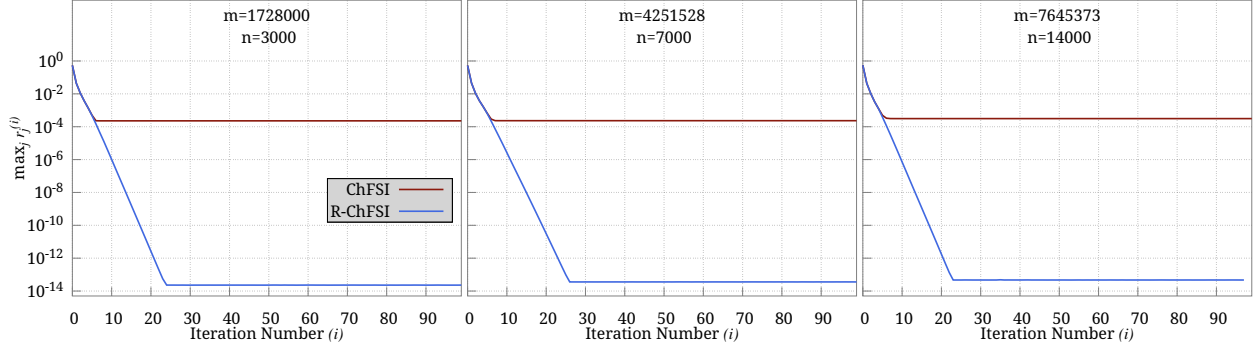


Figure 10: Plot of $\max_j r_j^{(i)} = \max_j \|\mathbf{A}\mathbf{x}_j^{(i)} - \epsilon_j^{(i)}\mathbf{B}\mathbf{x}_j^{(i)}\|$ as the iterations progress for the ChFSI method and the R-ChFSI method to solve the Hermitian generalized eigenvalue problem for the benchmark systems described in Table 1.

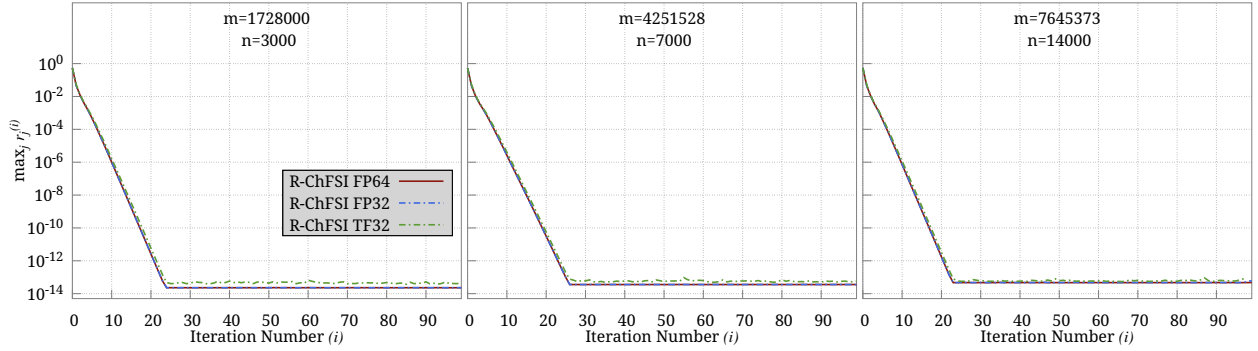


Figure 11: Plot of $\max_j r_j^{(i)} = \max_j \|\mathbf{A}\mathbf{x}_j^{(i)} - \epsilon_j^{(i)}\mathbf{B}\mathbf{x}_j^{(i)}\|$ as the iterations progress for the R-ChFSI method to solve the Hermitian generalized eigenvalue problem with various precisions for the benchmark systems described in Table 1.

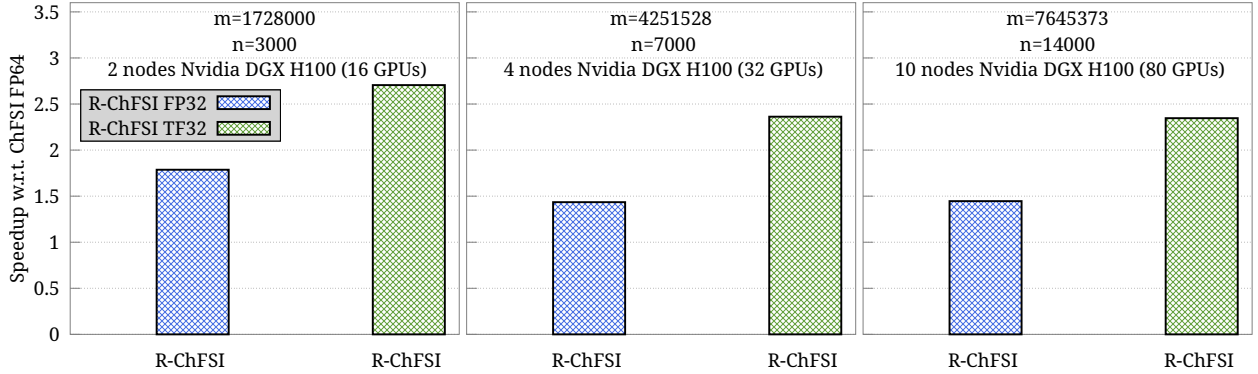


Figure 12: Speedups of lower precision R-ChFSI methods over the FP64 R-ChFSI method for subspace construction to solve the Hermitian generalized eigenvalue problem for the benchmark systems described in Table 1.

5. Conclusion

In this work, we presented a residual-based Chebyshev filtered subspace iteration (R-ChFSI) method tailored for large sparse Hermitian eigenvalue problems while being tolerant to inexact matrix-vector products.

We have demonstrated that the proposed method significantly outperforms the standard Chebyshev filtered subspace iteration (ChFSI) approach through extensive analysis and numerical experiments. We have provided a mathematical justification demonstrating that this reformulation reduces the numerical error in the Chebyshev filtered subspace construction while employing inexact matrix-vector products compared to the traditional ChFSI recurrence relation. We have studied the performance and accuracy of R-ChFSI under different computational precisions, demonstrating that it maintains robust convergence properties even when using lower-precision arithmetic. This characteristic makes it particularly suitable for modern hardware architectures that prioritize low-precision operations for efficiency gains in AI training. The results indicate that R-ChFSI achieves similar residual tolerances as full-precision ChFSI while retaining the performance benefits of reduced precision arithmetic.

For standard eigenvalue problems, we demonstrate that the proposed R-ChFSI method leverages the advantages of low-precision arithmetic. This capability is critical in today’s computational landscape, where the use of low-precision arithmetic (e.g., FP32, TF32) on modern hardware accelerators can dramatically reduce computational costs while the proposed R-ChFSI method still allows us to achieve high accuracy. Our benchmarks demonstrate that, for large-scale eigenproblems, R-ChFSI attains residual norms in the range of 10^{-12} to 10^{-14} which is a significant improvement over traditional ChFSI methods, that stagnate at residuals around 10^{-6} when using lower precision. In the context of generalized eigenvalue problems of the form $\mathbf{Ax} = \lambda\mathbf{Bx}$, the proposed R-ChFSI method is particularly impactful due to its ability to incorporate approximate inverses of \mathbf{B} . By replacing the exact computation of matrix inverses with computationally inexpensive approximate inverses (e.g., diagonal or block-diagonal approximations of \mathbf{B}), the method not only reduces the overall computational burden but also maintains convergence robustness. This results in substantial performance gains, as the proposed approach achieves residual tolerances that are up to ten orders of magnitude lower than those obtainable with traditional ChFSI when solving generalized problems. We further note that even in the context of generalized eigenvalue problems, the proposed R-ChFSI method allows us to utilize low-precision arithmetic alongside approximate inverses, further enhancing the computational gains.

The proposed R-ChFSI method is particularly relevant for quantum mechanics and material science applications, where we encounter large-scale sparse Hermitian eigenvalue problems. By enabling the use of lower-precision arithmetic without compromising accuracy, the proposed method provides an efficient alternative for large-scale simulations that require extensive computational resources. The ability to retain accuracy comparable to full precision solvers with reduced precision arithmetic further facilitates integration with modern accelerators, such as GPUs and specialized tensor-processing hardware. The findings in this study open avenues for further optimization and application of R-ChFSI in large-scale scientific computing tasks, including electronic structure calculations and other domains requiring efficient sparse eigenvalue solvers.

6. Acknowledgements

The authors gratefully acknowledge the seed grant from the Indian Institute of Science and the SERB Startup Research Grant from the Department of Science and Technology India (Grant Number: SRG/2020/002194). P.M. acknowledges Prathu Tiwari at Nvidia, Bangalore, for helping us run the benchmarks on NVIDIA DGX SuperPOD Eos system. The research also used the resources of PARAM Pravega at the Indian Institute of Science, supported by the National Supercomputing Mission (NSM) for testing few of the benchmarks on CPUs. N.K and K.R would like to acknowledge the Prime Minister Research Fellowship(PMRF) from the Ministry of Education India for financial support. P.M. acknowledges the Google India Research Award 2023 for financial support during the course of this work.

References

- [1] D. J. Griffiths, D. F. Schroeter, Introduction to Quantum Mechanics, Cambridge University Press, 2018. doi:10.1017/9781316995433.
- [2] L. Meirovitch, R. Parker, Fundamentals of Vibrations, Applied Mechanics Reviews 54 (2001) B100–B101. URL: <https://asmedigitalcollection.asme.org/appliedmechanicsreviews/article/54/6/B100/458203/Fundamentals-of-Vibrations>. doi:10.1115/1.1421112.
- [3] A. K. Chopra, Dynamics of structures: theory and applications to earthquake engineering, Prentice Hall international series in civil engineering and engineering mechanics, 3. ed ed., Pearson/Prentice Hall, Upper Saddle River, N.J, 2007.
- [4] K. Ogata, Modern control engineering, 5 ed., Prentice Hall, 2022. OCLC: 1492322544.
- [5] P. G. Drazin, W. H. Reid, Hydrodynamic Stability, 2 ed., Cambridge University Press, 2004. URL: <https://www.cambridge.org/core/product/identifier/9780511616938/type/book>. doi:10.1017/CB09780511616938.
- [6] P. M. Morse, K. U. Ingard, Theoretical acoustics, Princeton University Press, Princeton, N.J, 1986.
- [7] E. B. Wilson, J. C. Decius, P. C. Cross, Molecular vibrations: the theory of infrared and Raman vibrational spectra, Dover Publications, New York, 1980.
- [8] A. Szabo, N. S. Ostlund, Modern quantum chemistry: introduction to advanced electronic structure theory, Dover Publications, Inc, Mineola, New York, 2012.
- [9] C. M. Bishop, Pattern recognition and machine learning, Information science and statistics, Springer, New York, 2006.
- [10] F. R. K. Chung, Spectral graph theory, number no. 92 in Regional conference series in mathematics, Published for the Conference Board of the mathematical sciences by the American Mathematical Society, Providence, R.I, 1997.
- [11] C. D. Meyer, Matrix Analysis and Applied Linear Algebra, Second Edition, Society for Industrial and Applied Mathematics, Philadelphia, PA, 2023. URL: <https://epubs.siam.org/doi/book/10.1137/1.9781611977448>. doi:10.1137/1.9781611977448.
- [12] M. Crouzeix, B. Philippe, M. Sadkane, The Davidson Method, SIAM Journal on Scientific Computing 15 (1994) 62–76. URL: <http://epubs.siam.org/doi/10.1137/0915004>. doi:10.1137/0915004.
- [13] E. R. Davidson, The iterative calculation of a few of the lowest eigenvalues and corresponding eigenvectors of large real-symmetric matrices, Journal of Computational Physics 17 (1975) 87–94. URL: <https://linkinghub.elsevier.com/retrieve/pii/0021999175900650>. doi:10.1016/0021-9991(75)90065-0.
- [14] R. B. Morgan, D. S. Scott, Generalizations of Davidson’s Method for Computing Eigenvalues of Sparse Symmetric Matrices, SIAM Journal on Scientific and Statistical Computing 7 (1986) 817–825. URL: <http://epubs.siam.org/doi/10.1137/0907054>. doi:10.1137/0907054.

- [15] M. Hochstenbach, Y. Notay, The Jacobi–Davidson method, *GAMM-Mitteilungen* 29 (2006) 368–382. URL: <https://onlinelibrary.wiley.com/doi/10.1002/gamm.201490038>. doi:10.1002/gamm.201490038.
- [16] Y. Zhou, Y. Saad, M. L. Tiago, J. R. Chelikowsky, Self-consistent-field calculations using Chebyshev-filtered subspace iteration, *Journal of Computational Physics* 219 (2006) 172–184. doi:10.1016/J.JCP.2006.03.017, publisher: Academic Press.
- [17] A. V. Knyazev, Toward the Optimal Preconditioned Eigensolver: Locally Optimal Block Preconditioned Conjugate Gradient Method, *SIAM Journal on Scientific Computing* 23 (2001) 517–541. URL: <http://epubs.siam.org/doi/10.1137/S1064827500366124>. doi:10.1137/S1064827500366124.
- [18] E. Vecharynski, C. Yang, J. E. Pask, A projected preconditioned conjugate gradient algorithm for computing many extreme eigenpairs of a Hermitian matrix, *Journal of Computational Physics* 290 (2015) 73–89. URL: <https://linkinghub.elsevier.com/retrieve/pii/S002199911500100X>. doi:10.1016/j.jcp.2015.02.030.
- [19] W. E. Arnoldi, The principle of minimized iterations in the solution of the matrix eigenvalue problem, *Quarterly of Applied Mathematics* 9 (1951) 17–29. URL: <https://www.ams.org/qam/1951-09-01/S0033-569X-1951-42792-9/>. doi:10.1090/qam/42792.
- [20] C. Lanczos, An iteration method for the solution of the eigenvalue problem of linear differential and integral operators, *Journal of Research of the National Bureau of Standards* 45 (1950) 255. URL: https://nvlpubs.nist.gov/nistpubs/jres/045/jresv45n4p255_A1b.pdf. doi:10.6028/jres.045.026.
- [21] D. C. Sorensen, Implicit Application of Polynomial Filters in a k -Step Arnoldi Method, *SIAM Journal on Matrix Analysis and Applications* 13 (1992) 357–385. URL: <http://epubs.siam.org/doi/10.1137/0613025>. doi:10.1137/0613025.
- [22] G. W. Stewart, A Krylov–Schur Algorithm for Large Eigenproblems, *SIAM Journal on Matrix Analysis and Applications* 23 (2002) 601–614. URL: <http://epubs.siam.org/doi/10.1137/S0895479800371529>. doi:10.1137/S0895479800371529.
- [23] Y. Saad, *Numerical Methods for Large Eigenvalue Problems*, Society for Industrial and Applied Mathematics, 2011. doi:10.1137/1.9781611970739.
- [24] G. Kresse, J. Furthmüller, Efficiency of ab-initio total energy calculations for metals and semiconductors using a plane-wave basis set, *Computational Materials Science* 6 (1996) 15–50. doi:10.1016/0927-0256(96)00008-0.
- [25] R. Badeau, B. David, G. Richard, Fast approximated power iteration subspace tracking, *IEEE Transactions on Signal Processing* 53 (2005) 2931–2941. URL: <http://ieeexplore.ieee.org/document/1468483/>. doi:10.1109/TSP.2005.850378.
- [26] X. G. Doukopoulos, G. V. Moustakides, Fast and Stable Subspace Tracking, *IEEE Transactions on Signal Processing* 56 (2008) 1452–1465. URL: <http://ieeexplore.ieee.org/document/4471878/>. doi:10.1109/TSP.2007.909335.
- [27] C. Davila, Efficient, high performance, subspace tracking for time-domain data, *IEEE Transactions on Signal Processing* 48 (2000) 3307–3315. URL: <http://ieeexplore.ieee.org/document/886994/>. doi:10.1109/78.886994.
- [28] T. T. Ngo, Y. Saad, Scaled gradients on Grassmann manifolds for matrix completion, in: *Proceedings of the 26th International Conference on Neural Information Processing Systems - Volume 1*, volume 1 of *NIPS'12*, Curran Associates Inc., Red Hook, NY, USA, 2012, pp. 1412–1420.
- [29] H. Rutishauser, Simultaneous iteration method for symmetric matrices, *Numerische Mathematik* 16 (1970) 205–223. URL: <http://link.springer.com/10.1007/BF02219773>. doi:10.1007/BF02219773.
- [30] C. H. Loh, Chebyshev filtering Lanczos’ process in the subspace iteration method, *International Journal for Numerical Methods in Engineering* 20 (1984) 182–186. URL: <https://onlinelibrary.wiley.com/doi/10.1002/nme.1620200114>. doi:10.1002/nme.1620200114.
- [31] Y. Zhou, Y. Saad, M. L. Tiago, J. R. Chelikowsky, Parallel self-consistent-field calculations via Chebyshev-filtered subspace acceleration, *Physical Review E* 74 (2006) 066704. URL: <https://link.aps.org/doi/10.1103/PhysRevE.74.066704>. doi:10.1103/PhysRevE.74.066704, publisher: American Physical Society.
- [32] P. Motamarri, M. Nowak, K. Leiter, J. Knap, V. Gavini, Higher-order adaptive finite-element methods for Kohn–Sham

- density functional theory, *Journal of Computational Physics* 253 (2013) 308–343. URL: <https://linkinghub.elsevier.com/retrieve/pii/S0021999113004774>. doi:10.1016/j.jcp.2013.06.042.
- [33] A. Levitt, M. Torrent, Parallel eigensolvers in plane-wave Density Functional Theory, *Computer Physics Communications* 187 (2015) 98–105. doi:10.1016/j.cpc.2014.10.015.
- [34] Y. Zhou, Y. Saad, A Chebyshev–Davidson Algorithm for Large Symmetric Eigenproblems, *SIAM Journal on Matrix Analysis and Applications* 29 (2007) 954–971. URL: <http://epubs.siam.org/doi/10.1137/050630404>. doi:10.1137/050630404.
- [35] C.-Q. Miao, On Chebyshev–Davidson Method for Symmetric Generalized Eigenvalue Problems, *Journal of Scientific Computing* 85 (2020) 53. URL: <http://link.springer.com/10.1007/s10915-020-01360-4>. doi:10.1007/s10915-020-01360-4.
- [36] C.-Q. Miao, L. Cheng, On flexible block Chebyshev–Davidson method for solving symmetric generalized eigenvalue problems, *Advances in Computational Mathematics* 49 (2023) 78. URL: <https://link.springer.com/10.1007/s10444-023-10078-4>. doi:10.1007/s10444-023-10078-4.
- [37] B. Wang, H. An, H. Xie, Z. Mo, A new subspace iteration algorithm for solving generalized eigenvalue problems in vibration analysis, *Journal of Computational and Applied Mathematics* 468 (2025) 116622. URL: <https://linkinghub.elsevier.com/retrieve/pii/S0377042725001372>. doi:10.1016/j.cam.2025.116622.
- [38] S. Das, P. Motamarri, V. Subramanian, D. M. Rogers, V. Gavini, DFT-FE 1.0: A massively parallel hybrid CPU-GPU density functional theory code using finite-element discretization, *Computer Physics Communications* 280 (2022) 108473. URL: <https://linkinghub.elsevier.com/retrieve/pii/S0010465522001928>. doi:10.1016/j.cpc.2022.108473, publisher: North-Holland.
- [39] S. Ghosh, P. Suryanarayana, SPARC: Accurate and efficient finite-difference formulation and parallel implementation of Density Functional Theory: Extended systems, *Computer Physics Communications* 216 (2017) 109–125. doi:10.1016/j.cpc.2017.02.019.
- [40] Y. Zhou, J. R. Chelikowsky, Y. Saad, Chebyshev-filtered subspace iteration method free of sparse diagonalization for solving the Kohn–Sham equation, *Journal of Computational Physics* 274 (2014) 770–782. URL: <https://www.sciencedirect.com/science/article/pii/S0021999114004744>. doi:<https://doi.org/10.1016/j.jcp.2014.06.056>.
- [41] J. Feng, L. Wan, J. Li, S. Jiao, X. Cui, W. Hu, J. Yang, Massively parallel implementation of iterative eigensolvers in large-scale plane-wave density functional theory, *Computer Physics Communications* 299 (2024) 109135. doi:10.1016/j.cpc.2024.109135.
- [42] S. Das, P. Motamarri, V. Gavini, B. Turcksin, Y. W. Li, B. Leback, Fast, Scalable and Accurate Finite-Element Based Ab Initio Calculations Using Mixed Precision Computing: 46 PFLOPS Simulation of a Metallic Dislocation System, in: *Proceedings of the International Conference for High Performance Computing, Networking, Storage and Analysis*, volume 11, ACM, New York, NY, USA, 2019, pp. 1–11. URL: <https://dl.acm.org/doi/10.1145/3295500.3357157>. doi:10.1145/3295500.3357157.
- [43] S. Das, B. Kanungo, V. Subramanian, G. Panigrahi, P. Motamarri, D. Rogers, P. M. Zimmerman, V. Gavini, Large-Scale Materials Modeling at Quantum Accuracy: Ab Initio Simulations of Quasicrystals and Interacting Extended Defects in Metallic Alloys, *International Conference for High Performance Computing, Networking, Storage and Analysis, SC (2023)*. doi:10.1145/3581784.3627037, publisher: IEEE Computer Society ISBN: 9798400701092.
- [44] NVIDIA, HGX AI Supercomputing Platform, 2025. URL: <https://www.nvidia.com/en-us/data-center/hgx/>.
- [45] J. Dongarra, J. Gunnels, H. Bayraktar, A. Haidar, D. Ernst, Hardware Trends Impacting Floating-Point Computations In Scientific Applications, 2024. URL: <https://arxiv.org/abs/2411.12090>, arXiv: 2411.12090.
- [46] A. Kashi, H. Lu, W. Brewer, D. Rogers, M. Matheson, M. Shankar, F. Wang, Mixed-precision numerics in scientific applications: survey and perspectives, 2025. URL: <https://arxiv.org/abs/2412.19322>, arXiv: 2412.19322.
- [47] E. Carson, N. Khan, Mixed Precision Iterative Refinement with Sparse Approximate Inverse Preconditioning, *SIAM Journal on Scientific Computing* 45 (2023) C131–C153. doi:10.1137/22M1487709.

- [48] A. Abdelfattah, H. Anzt, E. G. Boman, E. Carson, T. Cojean, J. Dongarra, A. Fox, M. Gates, N. J. Higham, X. S. Li, J. Loe, P. Luszczek, S. Pranesh, S. Rajamanickam, T. Ribizel, B. F. Smith, K. Swirydowicz, S. Thomas, S. Tomov, Y. M. Tsai, U. M. Yang, A survey of numerical linear algebra methods utilizing mixed-precision arithmetic, *The International Journal of High Performance Computing Applications* 35 (2021) 344–369. doi:10.1177/10943420211003313.
- [49] H. Anzt, J. Dongarra, G. Flegar, N. J. Higham, E. S. Quintana-Ortí, Adaptive precision in block-Jacobi preconditioning for iterative sparse linear system solvers, *Concurrency and Computation: Practice and Experience* 31 (2019). doi:10.1002/cpe.4460.
- [50] N. J. Higham, S. Pranesh, Exploiting Lower Precision Arithmetic in Solving Symmetric Positive Definite Linear Systems and Least Squares Problems, *SIAM Journal on Scientific Computing* 43 (2021) A258–A277. doi:10.1137/19M1298263.
- [51] N. J. Higham, T. Mary, Mixed precision algorithms in numerical linear algebra, *Acta Numerica* 31 (2022) 347–414. doi:10.1017/S0962492922000022.
- [52] M. Baboulin, A. Buttari, J. Dongarra, J. Kurzak, J. Langou, J. Langou, P. Luszczek, S. Tomov, Accelerating scientific computations with mixed precision algorithms, *Computer Physics Communications* 180 (2009) 2526–2533. doi:10.1016/j.cpc.2008.11.005.
- [53] D. Göddeke, R. Strzodka, S. Turek, Performance and accuracy of hardware-oriented native-, emulated- and mixed-precision solvers in FEM simulations, *International Journal of Parallel, Emergent and Distributed Systems* 22 (2007) 221–256. doi:10.1080/17445760601122076.
- [54] D. Kressner, Y. Ma, M. Shao, A mixed precision LOBPCG algorithm, *Numerical Algorithms* 94 (2023) 1653–1671. doi:10.1007/s11075-023-01550-9.
- [55] P. Motamarri, S. Das, S. Rudraraju, K. Ghosh, D. Davydov, V. Gavini, DFT-FE – A massively parallel adaptive finite-element code for large-scale density functional theory calculations, *Computer Physics Communications* 246 (2020) 106853. URL: <https://linkinghub.elsevier.com/retrieve/pii/S001046519302309>. doi:10.1016/j.cpc.2019.07.016, publisher: North-Holland.
- [56] Y. Saad, Chebyshev Acceleration Techniques for Solving Nonsymmetric Eigenvalue Problems, *Mathematics of Computation* 42 (1984) 567. doi:10.2307/2007602.
- [57] A. Dektor, P. DelMastro, E. Ye, R. V. Beeumen, C. Yang, Inexact subspace projection methods for low-rank tensor eigenvalue problems, 2025. URL: <http://arxiv.org/abs/2502.19578>. doi:10.48550/arXiv.2502.19578, arXiv:2502.19578 [math].
- [58] B. Zhang, X. Jing, Q. Xu, S. Kumar, A. Sharma, L. Erlandson, S. J. Sahoo, E. Chow, A. J. Medford, J. E. Pask, P. Suryanarayana, SPARC v2.0.0: Spin-orbit coupling, dispersion interactions, and advanced exchange–correlation functionals, *Software Impacts* 20 (2024) 100649. doi:10.1016/j.simpa.2024.100649.
- [59] S. Ghosh, P. Suryanarayana, SPARC: Accurate and efficient finite-difference formulation and parallel implementation of Density Functional Theory: Isolated clusters, *Computer Physics Communications* 212 (2017) 189–204. doi:10.1016/j.cpc.2016.09.020.
- [60] Q. Xu, A. Sharma, B. Comer, H. Huang, E. Chow, A. J. Medford, J. E. Pask, P. Suryanarayana, SPARC: Simulation Package for Ab-initio Real-space Calculations, *SoftwareX* 15 (2021) 100709. doi:10.1016/j.softx.2021.100709.
- [61] L. Kronik, A. Makmal, M. L. Tiago, M. M. G. Alemany, M. Jain, X. Huang, Y. Saad, J. R. Chelikowsky, PARSEC – the pseudopotential algorithm for real-space electronic structure calculations: recent advances and novel applications to nano-structures, *physica status solidi (b)* 243 (2006) 1063–1079. doi:10.1002/pssb.200541463.
- [62] K.-H. Liou, C. Yang, J. R. Chelikowsky, Scalable implementation of polynomial filtering for density functional theory calculation in PARSEC, *Computer Physics Communications* 254 (2020) 107330. doi:10.1016/j.cpc.2020.107330.
- [63] J. Winkelmann, P. Springer, E. D. Napoli, ChASE, *ACM Transactions on Mathematical Software* 45 (2019) 1–34. doi:10.1145/3313828.
- [64] V. Michaud-Rioux, L. Zhang, H. Guo, RESCU: A real space electronic structure method, *Journal of Computational*

- Physics 307 (2016) 593–613. doi:10.1016/j.jcp.2015.12.014.
- [65] M. Dogan, K.-H. Liou, J. R. Chelikowsky, Solving the electronic structure problem for over 100 000 atoms in real space, *Physical Review Materials* 7 (2023) L063001. URL: <https://link.aps.org/doi/10.1103/PhysRevMaterials.7.L063001>. doi:10.1103/PhysRevMaterials.7.L063001.
- [66] Y. Chen, Y. Chi, J. Fan, C. Ma, Spectral Methods for Data Science: A Statistical Perspective, *Foundations and Trends® in Machine Learning* 14 (2021) 566–806. doi:10.1561/22000000079.
- [67] P. Zhu, A. Knyazev, Angles between subspaces and their tangents, *Journal of Numerical Mathematics* 21 (2013). doi:10.1515/jnum-2013-0013.
- [68] D. S. Watkins, *The Matrix Eigenvalue Problem*, Society for Industrial and Applied Mathematics, 2007. doi:10.1137/1.9780898717808.
- [69] N. J. Higham, *Accuracy and Stability of Numerical Algorithms*, Society for Industrial and Applied Mathematics, 2002. doi:10.1137/1.9780898718027.
- [70] H. Chen, X. Dai, X. Gong, L. He, A. Zhou, Adaptive Finite Element Approximations for Kohn–Sham Models, *Multiscale Modeling & Simulation* 12 (2014) 1828–1869. doi:10.1137/130916096.
- [71] V. Schauer, C. Linder, All-electron Kohn–Sham density functional theory on hierarchic finite element spaces, *Journal of Computational Physics* 250 (2013) 644–664. doi:10.1016/j.jcp.2013.04.020.
- [72] E. Tsuchida, M. Tsukada, Adaptive finite-element method for electronic-structure calculations, *Physical Review B - Condensed Matter and Materials Physics* 54 (1996) 7602–7605. doi:10.1103/PhysRevB.54.7602.
- [73] E. Tsuchida, M. Tsukada, Electronic-structure calculations based on the finite-element method, *Physical Review B* 52 (1995) 5573–5578. doi:10.1103/PhysRevB.52.5573.
- [74] J. E. Pask, P. A. Sterne, Finite element methods in *ab initio* electronic structure calculations, *Modelling and Simulation in Materials Science and Engineering* 13 (2005) R71–R96. doi:10.1088/0965-0393/13/3/R01.